

A Dominant Point Mutation in a RINGv E3 Ubiquitin Ligase Homoeologous Gene Leads to Cleistogamy in *Brassica napus*

Yun-Hai Lu,^a Dominique Arnaud,^a Harry Belcram,^a Cyril Falentin,^b Patricia Rouault,^b Nathalie Piel,^b Marie-Odile Lucas,^b Jérémy Just,^a Michel Renard,^b Régine Delourme,^b and Boulos Chalhoub^{a,1}

^aUnité de Recherche en Génomique Végétale (Institut National de la Recherche Agronomique, Centre National de la Recherche Scientifique, Université d'Evry Val d'Essonne), Organization and Evolution of Plant Genomes, 91057 Evry cedex, France

^bInstitut National de la Recherche Agronomique, Unité Mixte de Recherche 1349 Institut de Génétique, Environnement et Protection des Plantes, F-35653 Le Rheu, France

In the allopolyploid *Brassica napus*, we obtained a petal-closed flower mutation by ethyl methanesulfonate mutagenesis. Here, we report cloning and characterization of the *Bn-CLG1A* (*CLG* for cleistogamy) gene and the *Bn-clg1A-1D* mutant allele responsible for the cleistogamy phenotype. *Bn-CLG1A* encodes a RINGv E3 ubiquitin ligase that is highly conserved across eukaryotes. In the *Bn-clg1A-1D* mutant allele, a C-to-T transition converts a Pro at position 325 to a Leu (P325L), causing a dominant mutation leading to cleistogamy. *B. napus* and *Arabidopsis thaliana* plants transformed with a *Bn-clg1A-1D* allele show cleistogamous flowers, and characterization of these flowers suggests that the *Bn-clg1A-1D* mutation causes a pronounced negative regulation of cutin biosynthesis or loading and affects elongation or differentiation of petal and sepal cells. This results in an inhibition or a delay of petal development, leading to folded petals. A homoeologous gene (*Bn-CLG1C*), which shows 99.5% amino acid identity and is also constitutively and equally expressed to the wild-type *Bn-CLG1A* gene, was also identified. We showed that P325L is not a loss-of-function mutation and did not affect expression of *Bn-clg1A-1D* or *Bn-CLG1C*. Our findings suggest that P325L is a gain-of-function semidominant mutation, which led to either hyper- or neofunctionalization of a redundant homoeologous gene.

INTRODUCTION

The rapid explosion in diversity that followed the emergence of flowering plants in the early Cretaceous, ~130 million years ago, may be linked to the evolution of their reproductive organs, the flowers (Carroll, 2001). Cleistogamy, characterized by closed flowers that are self-pollinated and can produce fruits and seeds as a result of autogamy, contrasts with chasmogamy, characterized by opened flowers that can be cross-pollinated and produce fruits and seeds by allogamy (Uphof, 1938; Lord, 1981; Culley and Klooster, 2007). Darwin (1877) first reported cleistogamy as a common phenomenon widely distributed among the angiosperms and likely to have evolved from chasmogamy to ensure seed set by selfing. Cleistogamy is widespread and has been reported in at least 693 angiosperm species from 228 genera and 50 families (Culley and Klooster, 2007). There is no unique feature of cleistogamy, but it can be classified into three categories (reviewed in Culley and Klooster, 2007): dimorphic

cleistogamy, in which prominent floral differences in cleistogamy and chasmogamy floral morphology result from divergent developmental pathways; complete cleistogamy, in which individual plants produce only cleistogamous flowers; and induced cleistogamy, in which the environment arrests the development of chasmogamous flowers prior to anthesis and results in a mechanical failure of the flowers to open.

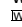
Although cleistogamy leads to inbreeding depression, it also may be advantageous for plants (reviewed in Culley and Klooster, 2007). The advantages include reproductive assurance (e.g., when pollinators are rare) and reduced resources needed for reproduction (Schemske, 1978; Waller, 1984). From a practical point of view, the cleistogamy trait could be useful in maintaining genetic purity (Saxena et al., 1993) and in developing genetically modified (GM) cultivars with low risk of gene flow to non-GM varieties (Kwon et al., 2001; Daniell, 2002; Lu, 2003).

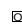
Genetic control of cleistogamy has been studied in several species. Lord (1981) suggested that the chasmogamy/cleistogamy might be under the control of polygenic inheritance and potentially readily modified by the environment in some studied species. Two or more independent genes were found to be responsible for cleistogamy in sorghum (*Sorghum bicolor*) (Merwin et al., 1981), soybean (*Glycine max*) (Takahashi et al., 2001), and barley (*Hordeum vulgare*) (Kurauchi et al., 1993; Turuspekov et al., 2004). Single recessive genes were found to be responsible for the cleistogamous trait in pigeon pea (*Cajanus cajan*; Saxena et al., 1992, 1993), durum wheat (*Triticum durum*; Chhabra and Sethi, 1991), and rice (*Oryza sativa*; Maeng et al., 2006). Recently, the

¹ Address correspondence to chalhoub@evry.inra.fr.

The author responsible for distribution of materials integral to the findings presented in this article in accordance with the policy described in the Instructions for Authors (www.plantcell.org) is: Boulos Chalhoub (chalhoub@evry.inra.fr).

 Some figures in this article are displayed in color online but in black and white in the print edition.

 Online version contains Web-only data.

 Open Access articles can be viewed online without a subscription.

www.plantcell.org/cgi/doi/10.1105/tpc.112.104315

barley *Cleistogamy1* gene (*Cly1*) was isolated by positional cloning (Nair et al., 2010). *Cly1* was found to be a homolog of the *Arabidopsis thaliana* transcription factor *APETALA2*, and the cleistogamous flowering phenotype was suggested to be caused by a mutation at the microRNA (miR172) targeting site that suppressed miR172-guided mRNA cleavage (Nair et al., 2010).

Oilseed rape (*Brassica napus*) is an economically important crop, cultivated worldwide for human consumption (third most important vegetable oil source after soybean and palm oil), animal feeding, and biodiesel. The genome of oilseed rape (AACC, $2n = 38$) is a recent amphitetraploid, derived from interspecific hybridization between *Brassica oleracea* (CC, $2n = 18$) and *Brassica rapa* (AA, $2n = 20$). The vast majority of cultivated oilseed rape cultivars are self-compatible and allogamous, with an outcrossing rate ranging between 12 and 55% (average 30%), depending on the genotype and environmental conditions (Beckie et al., 2003), although both of its diploid progenitors are self-incompatible (Silva and Goring, 2001). *B. napus* can disseminate its pollen as well as receive pollen from quite distantly related plants, including wild related species (Jørgensen and Andersen, 1994; Halfhill et al., 2002; Warwick et al., 2003; Ammitzbøll and Bagger Jørgensen, 2006; Ford et al., 2006; Song et al., 2010).

An oilseed rape mutant phenotype with flowers that do not open, leading to cleistogamy, was obtained in the early seventies by ethyl methanesulfonate (EMS) mutagenesis of seeds of the 'Primor' cultivar (Renard and Tanguy, 1997; Figure 1). The mutant plants 'Primor-*Clg*' (*Clg* stands for cleistogamy) develop and reproduce normally while having closed flowers (Figures 1B and 1E). Cleistogamous oilseed rape lines bred from this mutant were shown to have an autogamy rate as high as 94% and to

emit 10 times less pollen than an open-flowered oilseed rape in the same growing conditions (Fargue et al., 2006). No differences in seed production were observed between cleistogamous mutants and wild-type plants, indicating that fertility is not affected in cleistogamous oilseed rape (Renard and Tanguy, 1997; Fargue et al., 2006). This induced cleistogamous trait would be useful in oilseed rape breeding as it decreases the risk of genetic contamination and gene flow from GM varieties through outcrossing to other oilseed rape cultivars or to related *Brassica* species.

Here, we report the positional cloning and characterization of the gene responsible for this trait. We show that a single amino acid mutation in a highly conserved region of a RINGv E3 ubiquitin ligase homoeologous gene copy led to the cleistogamy phenotype in oilseed rape.

RESULTS

Phenotyping, Genetic Mapping, and Positional Cloning of the Cleistogamy Gene in *B. napus*

Cleistogamous oilseed rape showed a normal development compared with noncleistogamous plants. Cleistogamous flowers did not normally open at anthesis and remained closed, appearing like a big yellow bud until petal abscission (Figure 1). Other floral organs, such as carpel and stamens, develop normally. Notably, the cleistogamous character was shown to be variable where, depending on the genotype tested and environmental conditions, some flowers partially open, either showing a hole at the top of the bud permitting a partial extrusion of stamens

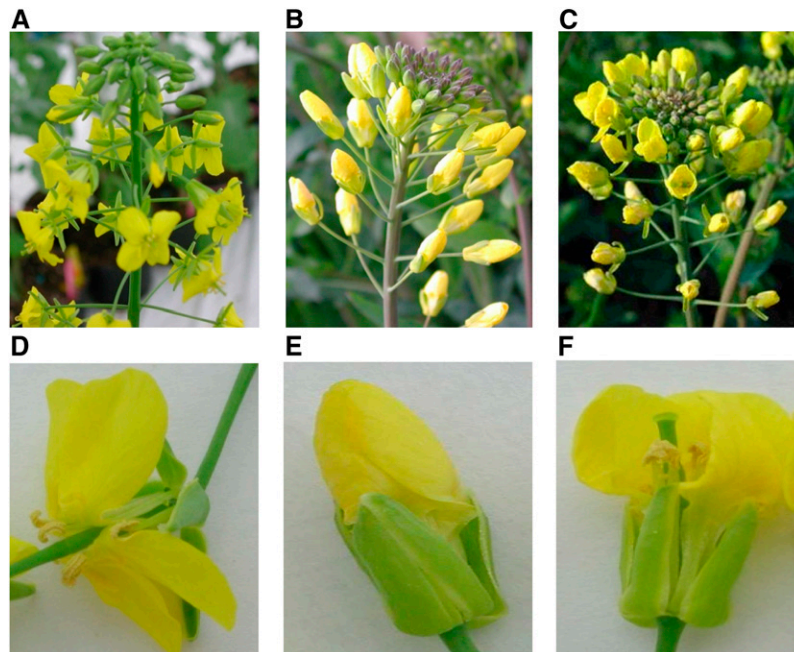


Figure 1. Oilseed rape (*Brassica napus*) flower morphology.

Normal noncleistogamous plants with open petals of cv Yudal (**[A]** and **[D]**), cleistogamous plants with closed petals of line B001-*Clg* (**[B]** and **[E]**), and intermediate-closed petals F1 plants (**[C]** and **[F]**).

or having one petal laterally malformed creating a slight gap between petals (Fargue et al., 2006; Figure 1; see Supplemental Figure 1 online). The cleistogamy trait has been successfully introgressed in several varieties where several pairs of cleistogamous/non-cleistogamous near-isogenic lines were produced (Renard and Tanguy, 1997).

Early genetic investigations showed that the cleistogamy phenotype in *B. napus* is controlled by a major locus called *Clg1* (Renard and Tanguy, 1997). F1 heterozygous plants show an intermediate phenotype with partially closed flowers (Renard and Tanguy, 1997; Figure 1C). In this study, we followed the international *Arabidopsis* and *Brassica* gene nomenclature and named the wild-type allele *CLG1A* and the mutant allele leading to cleistogamy as *clg1A-1D*. The letter A designates the genome on which the gene was mapped and the letter D the semidominant nature of the mutation. The prefixes Bn-, Br-, or Bo- were added to designate species names (*B. napus*, *B. rapa*, and *B. oleracea*, respectively) to avoid confusion when describing the different homologous

copies of the gene (see below). We initiated mapping of Bn-*CLG1A*/Bn-*clg1A-1D* using a segregating population of double haploid (DH) lines of a cross between the French cleistogamous line 'B001-*Clg*' and the genetically distant Korean cultivar 'Yudal.' The different steps of positional cloning are summarized in Figure 2 and detailed in Supplemental Results 1 online.

Briefly, the phenotyping of an initial population of 255 DH lines showed a segregation of 53% of noncleistogamous DH lines to 47% intermediate-cleistogamous and cleistogamous ones (see Supplemental Figure 1 online), fitting a monogenic model with the Bn-*clg1A-1D* allele leading to cleistogamy or partial cleistogamy. Initial molecular mapping was done with amplified fragment length polymorphism (AFLP) (Vos et al., 1995; Chalhoub et al., 1997) and allowed identification of five linked markers (Figure 2A). Sequencing of these AFLP markers and comparison with *Arabidopsis* genome sequence allow identification of a putative *Arabidopsis* orthologous genomic region on chromosome IV, based on high sequence homology of one AFLP marker sequence to the *At4g33760* gene of *Arabidopsis*. This was followed

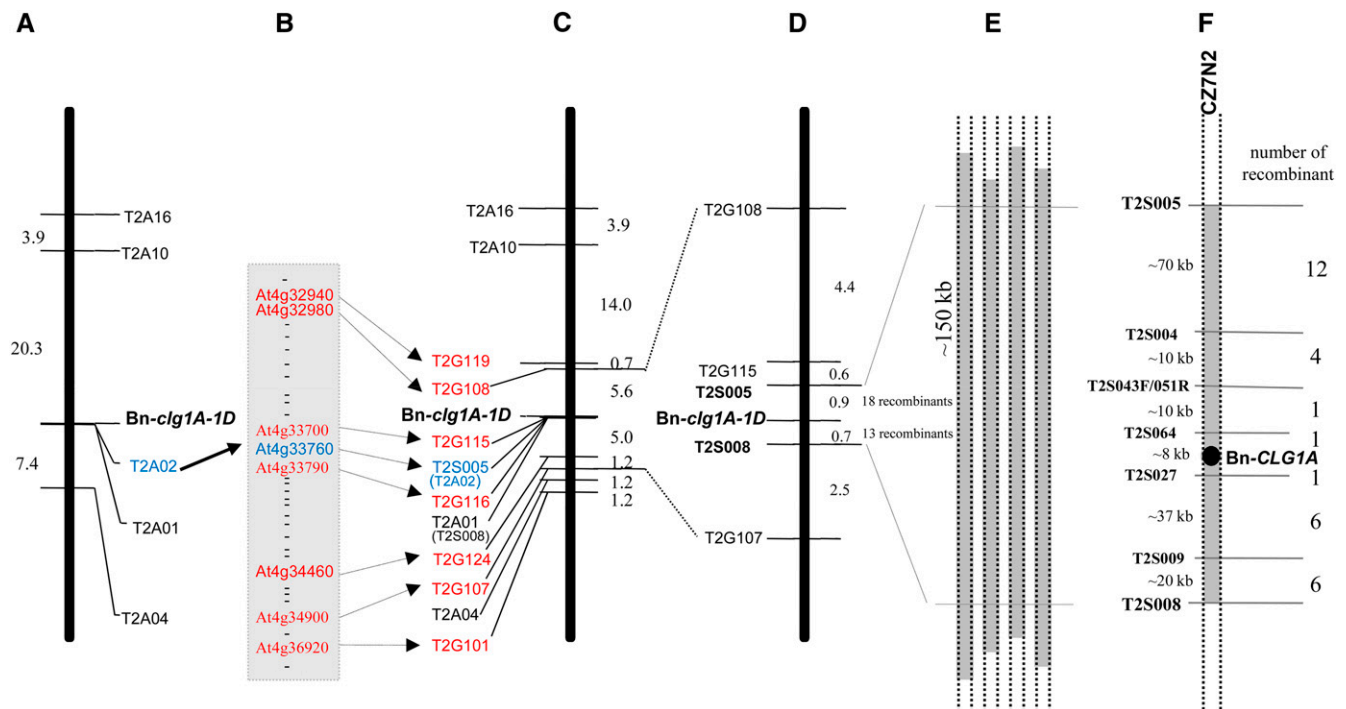


Figure 2. Mapping and Positional Cloning of Bn-*CLG1A*.

(A) Initial mapping of five AFLP markers on a population of 255 segregant DH lines derived from a cross between B001-*Clg* and cv Yudal. The genetic distance (centimorgans) between markers is shown on the left.

(B) Thirty-two *Arabidopsis* genes from a region of 2030 kb of chromosome IV around the *At4g33760* gene were used for generation of additional PCR markers.

(C) Seven genes (in addition to *At4g33760* gene) produced polymorphic PCR markers and were mapped around Bn-*clg1A-1D* on the same 255 DH segregating population.

(D) Finer genetic mapping of Bn-*clg1A-1D* on a larger DH population of 2158 lines.

(E) Identification of four BAC clones from Darmor-*bzh* BAC library, containing the closest flanking genetic markers: T2S005 and T2S008 and Bn-*CLG1A*.

(F) The BAC clone CZ7N2 was sequenced (237,660 bp) and shows that T2S005 and T2S008 delimit a region of 150 kb, whose sequence were used to generate five additional PCR markers. These were used to precisely locate Bn-*CLG1A*, using the 31 lines that show recombination between T2S005 and T2S008, to an ~8-kb interval containing a single candidate gene, encoding a putative RINGv E3 ubiquitin ligase.

by the use of 32 *Arabidopsis* gene sequences from this region to generate and map additional PCR markers (Figures 2B and 2C). Finer genetic mapping of *Bn-clg1A-1D* on a larger DH population of 2158 lines was then used to identify closely flanking markers (Figure 2D). The closest flanking genetic markers (T2S005 and T2S008) were used to screen a Darmor-*bzh* BAC library and four BAC clones that contain both markers, and thus the *Bn-CLG1A* wild-type allele, were identified (Figure 2E). One BAC clone (CZ7N2) was sequenced (237,660 bp) and compared with the *Arabidopsis* chromosome IV orthologous regions (See Supplemental Figure 2 and Supplemental Table 2 online). Analysis of the CZ7N2 BAC clone sequence showed that T2S005 and T2S008 delimit a region of 150 kb that was then used to generate five additional PCR genetic markers (Figure 2F). Mapping of these on 31 DH lines, which had a recombination between T2S005 and T2S008, delimited the *Bn-CLG1A* candidate region to an ~8-kb interval containing a single candidate gene that encodes a putative RINGv E3 ubiquitin ligase (Figure 2F).

Identification of the Causal Mutation by Comparison of the Mutant and Wild-Type Sequences

Sequence comparison of the 8-kb region spanning the *Bn-CLG1A* candidate gene between the wild and the EMS mutant cleistogamous lines was used to identify the causal mutation. As the *B. napus* genome is highly duplicated, to avoid artifacts related to simultaneous PCR amplification of homologous fragments and to directly access the genomic region of the mutant allele *Bn-clg1A-1D*, we constructed a pooled BAC library of the line 'Primor-*Clg*' as described by Isidore et al. (2005). Screening of the library with PCR markers linked to *Bn-clg1A-1D* identified three BAC clones that contain this mutant allele. After verification, one of the *clg1A*-carrying BAC clones (*Clg_H1B_P13a_3_J1*) was sequenced. The original *B. napus* cv Primor containing the wild-type *Bn-CLG1A* allele was used in the pedigree of the cv Darmor-*bzh* for which we have sequenced the BAC clone CZ7N2. Direct sequence comparison of *Bn-CLG1A* and *Bn-clg1A-1D* (CZ7N2 from Darmor-*bzh* and *Clg_H1B_P13a_3_J1* from 'Primor-*Clg*,' respectively) revealed three single nucleotide polymorphisms (SNPs) in a region of ~85 kb (see Supplemental Figure 3 online). Two of these were found in intergenic noncoding regions at ~10 kb (C-to-T) and ~35 kb (G-to-A), 5'- of the *Bn-CLG1A* candidate sequence (see Supplemental Figure 3 online). The third SNP mutation (C-to-T) was found inside the *Bn-CLG1A* candidate sequence, delimited by the closest flanking markers, T2S064 and T2S027. This SNP mutation occurs in the second exon of the predicted RING-finger protein gene and causes a substitution of Pro with a Leu at the position 325 (hereafter called P325L) in the protein sequence (see Supplemental Figure 3 online). Thus, comparative sequencing suggests that the P325L mutation in the gene encoding a putative RING-finger protein is the causal mutation leading to the cleistogamy trait.

Comapping between the Causal SNP and the Cleistogamy Phenotype

To confirm that the P325L mutation is responsible for the cleistogamous phenotype, we developed a cleaved amplified polymorphic

sequence (CAPS) marker (dCAPS-*Clg1*) which allows a clear distinction between wild-type and mutant alleles (see Supplemental Figure 4 online). The dCAPS-*Clg1* marker was completely linked to the cleistogamous phenotype with zero recombinant plants when analyzing the 'B001-*Clg*' × 'Yudal' DH lines segregating population of 255 lines and the 31 recombinant lines revealed from the larger 2158 segregating DH population. In particular, noncleistogamous DH lines (note 1) were shown to have the *Bn-CLG1A/Bn-CLG1A* genotype, whereas intermediate cleistogamous (noted 2 and 3) and cleistogamous DH lines (noted 4 and 5) have the genotype *Bn-clg1A/Bn-clg1A*. The dCAPS-*Clg1* marker also revealed a perfect association between the SNP type (T/C) and the corresponding cleistogamy phenotype on 19 pairs of near-isogenic lines for cleistogamy, as well as on 20 *B. napus* varieties (see Supplemental Figure 4B and Supplemental Table 3 online). No oilseed rape lines, in which cleistogamy trait was not introduced, were shown to carry this mutation (data not shown).

Bn-CLG1A Gene Structure

Sequence analysis predicted that *Bn-CLG1A* is 4144 bp in size and composed of nine exons interspersed by eight introns (Figure 3A). The predicted exon-intron structure was experimentally supported by sequencing of RT-PCR products obtained from flower buds as well as by the *B. napus* EST sequence data available in the National Center for Biotechnology Information public database.

The putative encoded protein is 1110 amino acids and has a predicted size of 123.05 kD (Figure 3A). Analysis of the *Bn-CLG1A* predicted protein sequence revealed the presence of several functional domains (Figure 3B): a RINGv protein domain at the N terminus (72 to 120, InterPro IPR011016); an adenylate cyclase-associated CAP_1 signature (293 to 305, InterPro IPR001837) located in a coiled-coil domain (294 to 321); a Leu zipper domain (800 to 821); and 14 transmembrane regions/helices (163 to 183, 202 to 222, 352 to 372, 464 to 484, 529 to 549, 575 to 595, 633 to 651, 703 to 723, 796 to 816, 844 to 864, 885 to 914, 928 to 948, 983 to 1003, and 1017 to 1037). The *Bn-CLG1A* protein sequence exhibits feature similarities with previously described RINGv E3 ubiquitin ligase protein in *Arabidopsis* (Kraft et al., 2005; Stone et al., 2005; Vierstra, 2009). A RING domain is required in interactions with substrate protein for E3 ligase activity by binding E2 (Lovering et al., 1993; Borden and Freemont, 1996; Borden, 2000). The encoded protein also contains other diverse protein-protein interaction domains that can serve as additional specific substrate binding sites of the E3 ligase. Internal domains, like the coiled-coil domain/CAP_1 signature and Leu zipper domain (Figure 3B), might function as a substrate binding domain of the *Bn-CLG1A* E3 ligase for specific substrate/target recognition (Lorick et al., 1999; Smalle and Vierstra, 2004). The point mutation at position 325 in the *Bn-clg1A* protein is located near the coiled-coil domain/CAP_1 domain and could thus modify the specificity of the substrate protein recognition or cofactor binding of the *Bn-clg1A* protein.

Further analysis of the predicted protein sequences (see Methods) shows that *Bn-CLG1A* is predicted to localize in the plasma membrane (WoLFPSORT and MultiLoc) and in plastids/chloroplasts (TargetP1.1, ChloroP 1.1, and TargetLoc), with

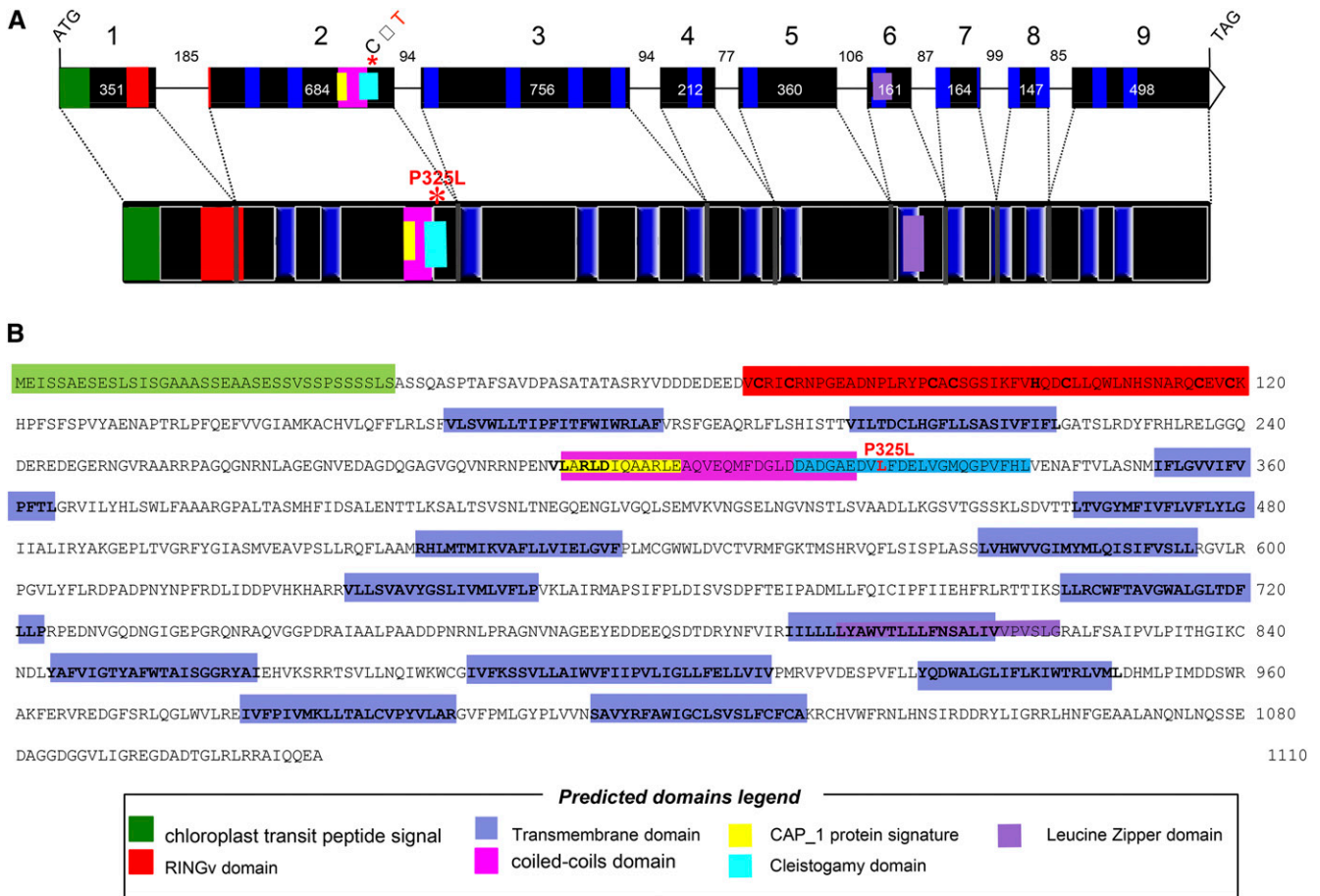


Figure 3. *B. napus* Cleistogamy (*Bn-CLG1A*) Gene Structure.

(A) Exon/intron structure of *Bn-CLG1A* with nine exons (black boxes) and eight introns with their corresponding sizes (in base pairs).
 (B) Deduced *Bn-CLG1A* mutant amino acid sequence.
 The different domains predicted by comparison with structure of homologs from different species are highlighted by same colored boxes in (A) and (B), and their legend is presented in the "predicted domains" box. The P325L cleistogamy mutation is highlighted in red.

a typical chloroplastic Ser-rich domain (von Heijne et al., 1989; Zybailov et al., 2008) at its N terminus (Figures 3A and 3B).

Identification of a Highly Conserved Redundant Homoeolog in *B. napus* and Identical Corresponding Orthologs in the Parental Species

Because *Brassica* species genomes are highly duplicated through recurrent polyploidy, it was important to understand the evolution of *Bn-CLG1A* duplicated copies for a better functional characterization.
 The predicted *Bn-CLG1A* protein shares a 90.5% amino acid identity and has similar intron/exon structure with the protein encoded by the *Arabidopsis* orthologous gene *At4g34100* (Figure 4), also predicted to be a RINGv E3 ubiquitin ligase family member (Stone et al., 2005). Interestingly, a recent study demonstrated that a mutant form of *At4g34100* corresponds to the wax mutant *eceriferum9*, which confers drought tolerance to *Arabidopsis* (Koornneef et al., 1989; Lü et al., 2012) (see Discussion). Analysis of the *Arabidopsis* genome did not identify another homolog of *At4g34100* on the *Arabidopsis* region that

resulted from the last alpha genome duplication (Schrantz and Mitchell-Olds, 2006) located on chromosome 2. A highly divergent paralogous copy (*At4g32670*), sharing only 23% amino acid similarity, was identified on chromosome 4, located at 576 kb from *At4g34100*. These two gene copies are both expressed in *Arabidopsis* (EST available in public databases). They both possess a conserved predicted RINGv domain at their N-terminal region but present different predicted membrane topology patterns. Like *At4g34100*, the *At4g32670* protein is predicted to be localized at the plasma membrane, but it does not contain a chloroplast targeting signal like *At4g34100* at its N terminus. The *At4g32670* protein is predicted by TargetP1.1 to have no chloroplast and no mitochondrial localization. So the two proteins should have diverged functions/roles in the cell and might have different proteins/substrates as targets for degradation.

Brassica species have undergone genome triplication, shortly after the divergence from *Arabidopsis*. Accordingly, compared with *Arabidopsis*, three homologous regions are expected in the genome of each of the *Brassica* diploid species (for example, *B. rapa* and *B. oleracea*) and up to six in the amphiploid *B. napus*

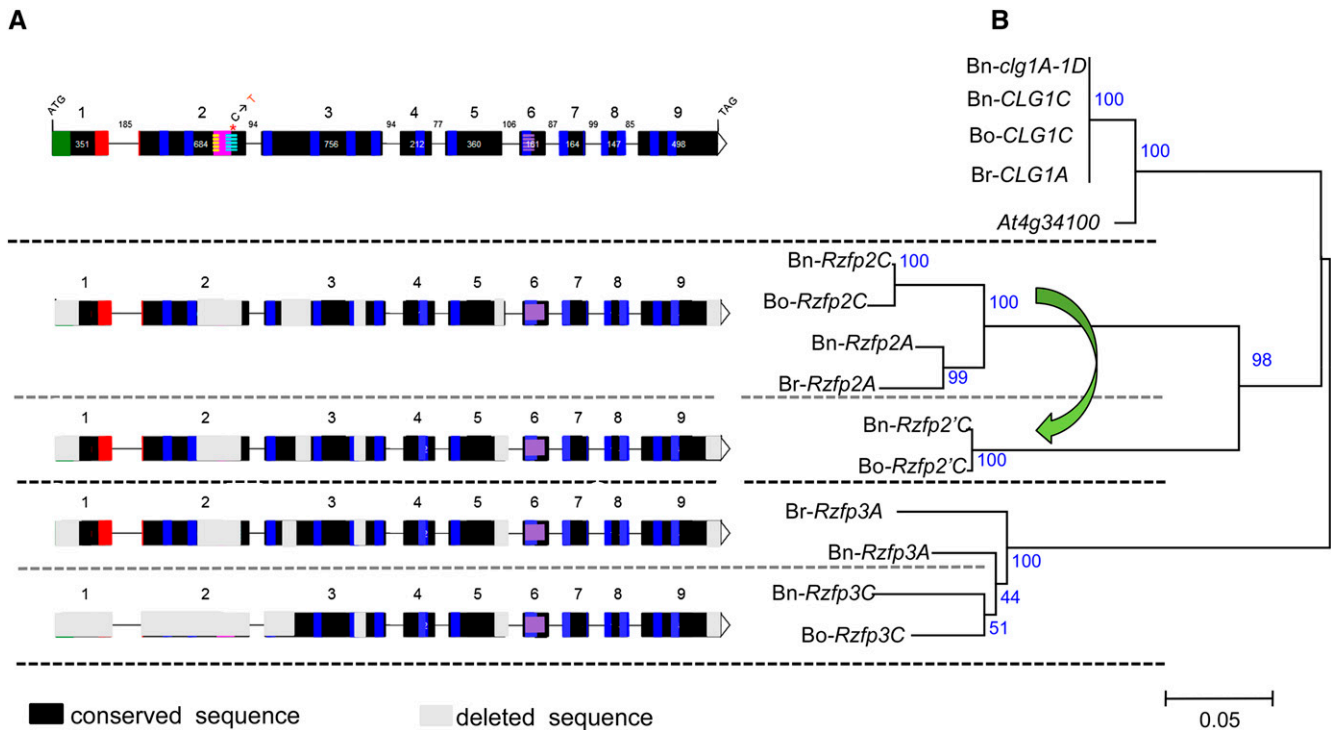


Figure 4. Gene Structure Comparison and Phylogenetic Analysis between Bn-CLG1A Homologs Identified in *B. napus*, *B. oleracea*, *B. rapa*, and *Arabidopsis*.

Gene structure comparison (**A**) and phylogenetic analysis (**B**). Deduced amino acid sequences of these homologs were aligned with ClustalX (Thompson et al., 1997). The phylogeny analysis was performed with MEGA version 4.1 using the neighbor-joining method (Tamura et al., 2007). The percentage of replicates trees in which the associated taxa clustered together in the bootstrap test (1000 replicates) are shown next to the branches. The legend of gene structure in (**A**) is the same as in Figure 3. The green arrow indicates tandem duplication of the *Rzfp2C* gene copy into *Rzfp2'C* in the C genome of *B. napus* (Bn-*Rzfp2'C*) and *B. oleracea* (Bo-*Rzfp2'C*). Rzfp, RING zinc finger protein.

(Parkin et al., 2005; Lysak et al., 2007). Direct comparison of the Bn-CLG1A sequence with the recently released genome sequence of *B. rapa* (Wang et al., 2011) allows identification of three homologous copies that resulted from the *Brassica* genome triplication (see Supplemental Figure 5A online). In comparison, four copies were found in the complete genome assembly of *B. oleracea* (<http://brassicadb.org/brad/>). Three of these result from the *Brassica* genome triplication and were orthologous to those of *B. rapa*, whereas the fourth copy located at 31 kb from one of the *B. oleracea* triplicated copies is derived from tandem duplication that occurred only in *B. oleracea* (Figure 4). As expected, seven copies were identified in *B. napus*, three on the A genome, orthologous to those identified in *B. rapa* and four on the C genomes, orthologous to those identified in *B. oleracea*.

Of these different *Brassica* homologs, only the orthologous copies from *B. rapa* (Br-CLG1A) and *B. oleracea* (Bo-CLG1C) and the homoeologous copy found on the C genomes of *B. napus* (Bn-CLG1C), are highly conserved where all protein domains described above can be found (Figure 4A). The *B. rapa* Br-CLG1A orthologous copy shows identical amino acid sequences to the Bn-CLG1A wild-type gene on the A genome of *B. napus* (Figure 4B). Similarly, the *B. oleracea* Bo-CLG1C copy shows identical amino acid sequences to the Bn-CLG1C orthologous copy identified on the C genome of *B. napus* (Figure 4B).

Comparisons between the A and C genomes show also that Bn-CLG1A/Br-CLG1A and Bn-CLG1C/Bo-CLG1C orthologous and homoeologous genes are highly similar (99.5 amino acid identity) (Figure 4B), with only two amino acid deletions and three other transitions in the C genome copies compared with the A ones. The other homologous copies were truncated in several of their exons and protein domains (Figure 4A), indicating important gene fractionations that have followed *Brassica* species genome triplication as previously reported (Wang et al., 2011; Cheng et al., 2012; Tang et al., 2012) and were grouped far from the Bn-CLG1A/Bo-CLG1A and Bn-CLG1C/Bo-CLG1C genes and their *Arabidopsis* At4g34100 ortholog (Figure 4B). Importantly, the cleistogamy domain found in Bn-CLG1A and its homoeologous and orthologous genes were also deleted in the remaining homologous copies (Figure 4A). Therefore, they were designated as RING zinc finger protein (*Rzfp*) coding gene homologs (Figure 4). The close evolutionary relationship of *Arabidopsis* orthologous genes with one of the *Brassica* homologs, derived from the genome triplication, which was closer than between the homologs themselves, was previously reported (Wang et al., 2011; Cheng et al., 2012; Tang et al., 2012). It is important to note that this close relationship between *Arabidopsis* and one of the three *Brassica* subgenomes does not constantly favor a specific subgenome, but rather switches among the three

subgenomes, depending on the considered gene, as we showed in the comparison of five genes that surround *Bn-CLG1A* in *B. rapa*, which are conserved as triplicates in *B. rapa* and are syntenic to *Arabidopsis* (see Supplemental Figure 5 online). Notably, this close relationship is relative because comparisons show that overall triplicated genes from *Brassica* and their *Arabidopsis* orthologs remain closer to each other than to *Bn-CLG1A* homologs from any other given species (data not shown). These observations may confirm that, in comparison to *Arabidopsis*, the three *Brassica* subgenomes reunited together through two steps of ancient allopolyploidy (Wang et al., 2011) would have undergone an accelerated and divergent fractionation of redundant genes, as suggested in previous studies (Wang et al., 2011; Cheng et al., 2012; Tang et al., 2012).

Bn-CLG1A Homologs in Other Plant and Eukaryote Species

In addition to *Arabidopsis* and other *Brassica* species, we identified, by BLASTp, tBLASTx, or tBLASTn, *Bn-CLG1A* homologous genes in various plant species (see Supplemental Table 4 online). Homologs were also identified in all other analyzed eukaryote species, including protists, fungi, algae, nematode, insects, fish, mouse, human, and yeast (*Saccharomyces cerevisiae*) (see Supplemental Table 4 online). No homologous sequence was found in prokaryotes (*Bacteria* or *Archaea*).

A phylogenetic tree of *Bn-CLG1A* homologous genes in plants was constructed using the protein sequences (Figure 5A). Another phylogenetic tree including all eukaryotes and showing the separation between plant and nonplant *Bn-CLG1A* homologs is presented in Supplemental Figure 6 online (See also Supplemental Data Set 2 online for sequence alignment.). In the rare cases where more than one copy was found in a specific genome, the copy most similar to *Bn-CLG1A* was selected for tree construction.

In the plant kingdom, the eudicot species were clearly distinguished from monocots and from the nonvascular plants, such as *Physcomitrella patens* (Figure 5A). *Bn-CLG1A* homologs in all studied eudicots contain a chloroplast/plastid targeting polypeptide signal in its N terminus (Figure 5B). By contrast, this domain was not found in the six grass monocot species and the nonvascular plant *P. patens* (Figure 5B). The corresponding N-terminal sequences of the *Bn-CLG1A* homologs in the two noneudicot angiosperm species (*Aquilegia coerulea* and *Amborella trichopoda*) and the two nongrass monocots (*Musa acuminata* and *Phoenix dactylifera*) did not align well with the chloroplast/plastid targeting polypeptide signal of eudicots (Figure 5B). Nevertheless, the *A. coerulea* noneudicot species and the *M. acuminata* nongrass monocots species are Ser rich (Figure 5B). Ser enrichment was suggested as an important, but not sufficient, feature of the chloroplast/plastid targeting polypeptide signal (von Heijne et al., 1989; Zybailov et al., 2008).

All identified *Bn-CLG1A* homologs share a similar transmembrane domain topology with 14 predicted transmembrane regions, as well as a highly conserved RINGv domain (C4HC3 type) with characteristic metal ligands (Figure 5C; see Supplemental Figure 7 online).

The *Bn-CLG1A* protein shares 24.3% amino acid sequence similarity with human TEB4p and 13.1% with yeast DOA10p, and TEB4p and DOA10p have 11.9% amino acid similarity with each other (Swanson et al., 2001; Hampton, 2002; Carvalho

et al., 2006; Kreft et al., 2006). Despite their sequence divergence, comparisons show a similar predicted transmembrane topology of *Bn-CLG1A*, TEB4p, and DOA10p (see Supplemental Figure 8 online). Both the N-terminal RINGv domain and the C terminus are predicted to be localized to the inner side of the membrane (~60% of protein is predicted to face the inner side and ~20% of protein to the outer side of the membrane) as in yeast and human homologs.

The cleistogamy-inducing point mutation P325L in *Bn-clg1A-1D* occurred in a 23-amino acid domain that is highly conserved in all analyzed plant species as well as in the nonvascular plant *P. patens* subsp *Patens* (Figure 5D). We named this the *cleistogamy* domain (Figure 5D).

Bn-CLG1A and Bn-CLG1C Homoeologous Genes Are Constitutively and Equally Expressed in *B. napus*

The expression pattern of *Bn-CLG1A* and *Bn-CLG1C*, highly conserved homoeologous gene copies, was first analyzed in *B. napus* by quantitative PCR using gene-specific primers on a wide panel of tissues and organs collected from the oilseed rape cultivar *Darmor-Bzh*. Both *Bn-CLG1A* and *Bn-CLG1C* homoeologs were constitutively and equally expressed in young leaves, petioles, stems, floral buds, and young siliques and immature seeds (Figure 6A). We observed a slight increase in the steady state level of *Bn-CLG1A* and *Bn-CLG1C* transcripts in roots (Figure 6A).

Expression of the *Bn-clg1A-1D* Mutant Allele Is Similar to the Wild-Type *Bn-CLG1A* and the Homoeologous *Bn-CLG1C*

To determine whether the expression of the *Bn-clg1A-1D* allele is affected, we compared the expression of wild-type *Bn-CLG1A* and *Bn-clg1A-1D* as well as the *Bn-CLG1C* homoeolog using quantitative PCR in young 3- or 5-mm flower buds of the two isogenic *B. napus* cultivars *Primor* and *Primor-Clg*. We found that the *Bn-clg1A-1D* mutant allele is expressed in *Primor-Clg* equally to the *Bn-CLG1A* wild-type allele in *Primor* (Figure 6B). Expression of the *Bn-CLG1C* homoeolog was also similar to *Bn-clg1A-1D* and *Bn-CLG1A* in both isogenic cultivars (Figure 6B).

We also analyzed *Bn-CLG1A* promoter activity in floral tissues using a reporter gene fusion construct. Thus, the 893-bp promoter fragment of *CLG1A* was inserted into the pBI101-GUS vector to produce the *pBn-CLG1A:GUS* construct (see Supplemental Figure 9 online), and β -glucuronidase (GUS) histochemical assays were performed on young and old floral buds of *B. napus* transgenic plants. Plants transformed with *pBn-CLG1A:GUS* showed that the transcriptional activity was high in the sepals of young floral buds (Figure 6C). In mature flowers, *Bn-CLG1A* promoter activity was stronger in sepals and anthers than in the style of pistils and the base of petal blades (Figure 6C).

B. napus Plants Transformed with the *Bn-clg1A-1D* Gene Exhibit a Cleistogamy Phenotype

To further validate the cleistogamy candidate gene, next recapitulated the cleistogamy mutant phenotype by transforming wild-type *B. napus* with the *clg1A* mutant genomic fragment. To

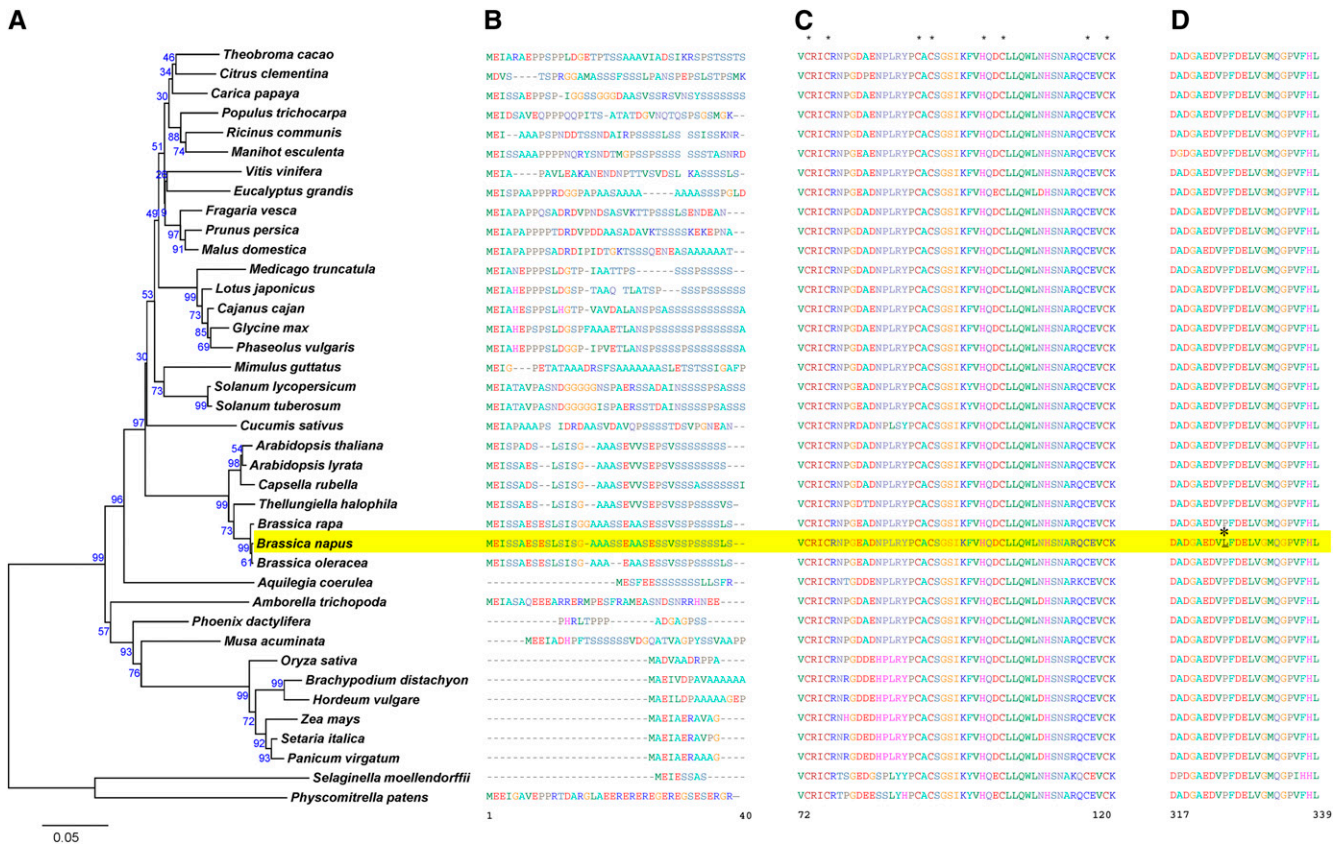


Figure 5. Phylogenetic analysis of plant homologs of Bn-CLG1A and amino acid sequence alignment of important domains.

Phylogenetic analysis was done with homologs of Bn-CLG1A from 39 plant species. **(A)** The chloroplast domain characterized by enrichment of the Ser amino acid **(B)**. The RINGv domain characterized by conserved eight metal ligands marked with an asterisk **(C)**. The highly conserved cleistogamy domain where the cleistogamy mutation P325L (asterisk) occurred in the *B. napus* Bn-*clg1A-1D* allele **(D)**. Amino acid sequences were aligned using ClustalX (Thompson et al., 1997). The phylogeny analysis was performed with MEGA version 4.1 using the neighbor-joining method (Tamura et al., 2007). The percentage of replicates in which the associated taxa clustered together in the bootstrap test (1000 replicates) is shown next to the branches. Amino acid numbering is presented according to the Bn-*clg1A-1D* sequences of *B. napus* (highlighted in yellow). (See Supplemental Data Set 1 online for sequence alignment.)

this end, we conducted *Agrobacterium tumefaciens*-mediated transformations of a noncleistogamous oilseed rape line cv Westar as well as an *Arabidopsis* line (Columbia-0 [Col-0]) with a Bn-*clg1A-1D*-derived construct to express the Bn-*clg1A-1D* allele under the control of its native promoter (see Methods and Supplemental Figure 9 online).

Of 18 kanamycin-resistant T1 transgenic *B. napus* plants, theoretically hemizygous for the transgene and homozygous for the wild-type Bn-CLG1A allele, six lines exhibited the wild-type opened flower phenotype and 12 lines showed an intermediate-cleistogamous phenotype. Three representative intermediate-cleistogamous *B. napus* transgenic (T1) plants are shown in Figure 7A. These transgenic plants develop normally and flower at a similar time to the control non-transgenic *B. napus* cv Westar. Compared with the control, all the intermediate-cleistogamous lines analyzed exhibited the same floral phenotype with apical floral buds completely closed, while opened or partly opened flowers were observed at the middle and the base of the stems, confirming that the

cleistogamy phenotype was caused by the induced P325L mutation (Figure 7A). Notably, few flowers were also observed and the cleistogamous phenotype observed for the *B. napus* Bn-*clg1A-1D* transgenic lines was less pronounced than the phenotype of the original Bn-*clg1A-1D* mutant line Primor-Clg or to the 'B001-Clg' line and more resembled the intermediate-cleistogamous phenotype described above (cf. Figures 1 and 7A).

Arabidopsis Plants Transformed with the Mutated Bn-*clg1A-1D* Gene Exhibit a Pronounced Cleistogamy Phenotype and Reduced Fertility

To get more insights into the function of the Bn-*clg1A-1D* allele, we next recapitulated the phenotype in *Arabidopsis* by expressing the same Bn-*clg1A* construct that worked in *B. napus*. We carefully analyzed the phenotype of three *Arabidopsis* independent T1 lines transformed with the Bn-*clg1A-1D* gene-derived construct as was used in *B. napus* (under the control of its native promoter). At the flowering stage, flowers of Bn-*clg1A-1D*

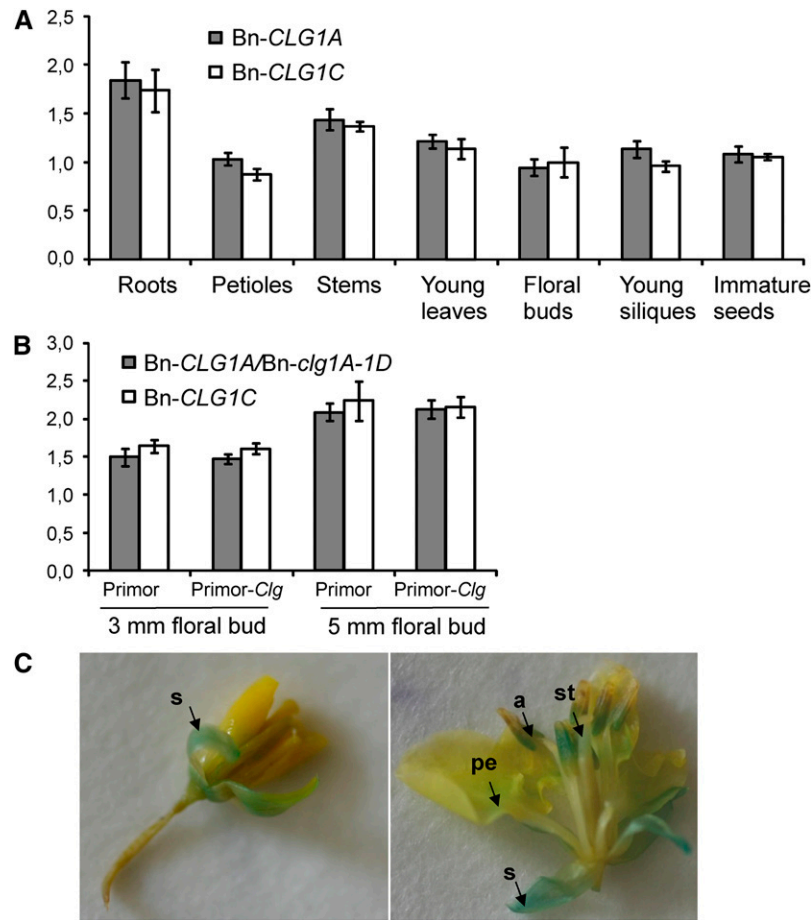


Figure 6. *Bn-clg1A-1D*, *Bn-CLG1A*, and *Bn-CLG1C* Homoeologs Are Constitutively and Similarly Expressed in *B. napus*.

(A) *Bn-CLG1A* and *Bn-CLG1C* expression levels in different tissues of *B. napus* cv Darmor. Transcript levels were determined by quantitative RT-PCR and normalized to both *EF-1* and *UBQ2* genes. Bars indicate *sd* ($n = 3$).

(B) *Bn-clg1A-1D* and *Bn-CLG1C* expression levels in *B. napus* cv Primor (the wild type) and Primor-*Clg* (*Bn-clg1A-1D* mutant) 3- and 5-mm floral buds. Transcript levels were determined by quantitative RT-PCR and normalized to both *EF-1* and *UBQ2*. Bars indicate *sd* ($n = 3$). The experiments have been repeated twice with similar results.

(C) GUS assay on young (left) and old (right) flowers of transgenic *B. napus* cv Westar transformed with the *pBn-CLG1A:GUS* construct. Arrows indicate the accumulation of GUS product (blue staining) in sepal (s), the base of petal (pe), anther (a), and style (st) of a developing flower. [See online article for color version of this figure.]

transgenic *Arabidopsis* were strongly cleistogamous with unopened floral buds (Figure 7B). Indeed, compared with the cleistogamous *B. napus* 'B001-*Clg*' line, the *Bn-clg1A-1D* transgenic *Arabidopsis* lines exhibited a more pronounced cleistogamous phenotype with more strongly closed flowers (Figures 7A and 7B). Terminal inflorescences of *Bn-clg1A-1D* transgenic *Arabidopsis* produced more floral buds and were more compact compared with the wild type (Figure 7B; see Supplemental Figures 10A and 10B online). In addition, apical floral buds appear glued between them.

In the *Bn-clg1A-1D* transgenic *Arabidopsis*, most of the siliques did not develop and the ones that developed were semi-sterile (see Supplemental Figure 10B online). Each line produced only one to five fully developed siliques that were curved, shorter, and wider compared with wild-type siliques (see Supplemental Figures 10D to 10F online). Notably, petals of *Bn-clg1A-1D*

transgenic *Arabidopsis* remain attached to siliques, whereas those of wild-type plants abscised normally (see Supplemental Figures 10D to 10F online).

***Bn-clg1A-1D* Transgenic *Arabidopsis* Plants Are Affected in Petal Epidermal Cell Elongation and Cuticular Nanoridge Deposition**

To further dissect the cleistogamous phenotype of T1 *Arabidopsis* plants transformed with *Bn-clg1A-1D*, floral buds and flowers were analyzed with a microscope or using a scanning electron microscope. Unopened floral buds of *Bn-clg1A-1D* transgenic *Arabidopsis* displayed organ fusions between sepals and between sepals and petals (Figures 8A and 8B; see Supplemental Figure 11 online). Compared with the wild type, petals of *Bn-clg1A-1D* *Arabidopsis* were folded, thicker, and

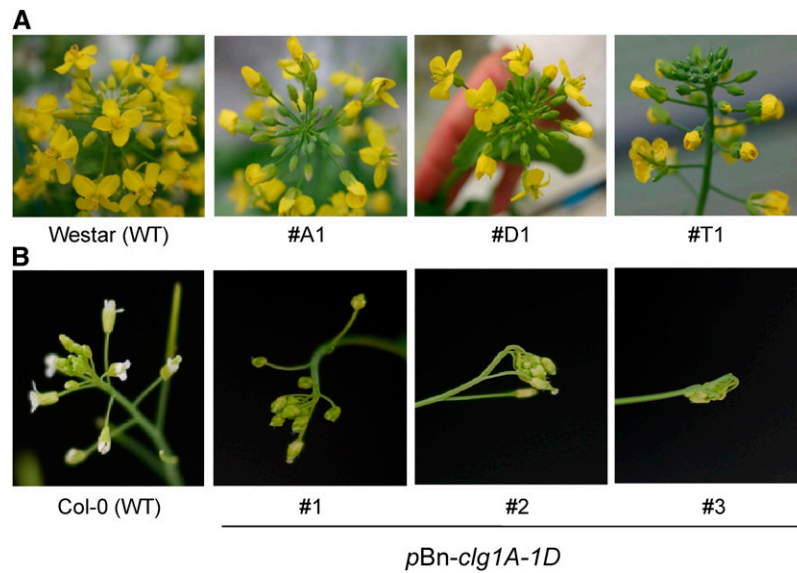


Figure 7. Cleistogamous Phenotypes of *B. napus* and *Arabidopsis* Plants Transformed with *Bn-clg1A-1D*.

(A) Inflorescence of *B. napus* cv Westar and three representative T0 transgenic lines (#T1, #D1, and #A1) of same cultivar transformed with the *pBn-clg1A-1D* construct. WT, the wild type.

(B) Inflorescence of *Arabidopsis* ecotype Col-0 (the wild type) and three independent *pBn-clg1A-1D* transgenic T0 lines (#1, #2, and #3) in the same ecotype (see Supplemental Figure 9 online for details of construct *pBn-clg1A-1D*).

cannot develop inside the closed flower (Figure 8; see Supplemental Figures 11A to 11D online). Elongation of carpel was restricted and they were curved or twisted (see Supplemental Figures 11C and 11D online).

In *Bn-clg1A-1D* transgenic *Arabidopsis*, epidermal cells at the base of petals were much less elongated than in wild-type plants, whereas the size of epidermal cells of the upper petal blade did not change compared with the wild type (see Supplemental Figures 11E and 11F online). As previously observed (Pyke and Page, 1998), these two types of epidermal cells each occupied about half of the petal length in the wild-type plant. Interestingly, in *Bn-clg1A-1D* transgenic *Arabidopsis*, the proportion of conical epidermal cells in the upper part of petals, especially the ones at the adaxial surface, was higher than the proportion of the thin and elongated epidermal cells at the base of petals (see Supplemental Figures 11E and 11F online). This result suggests that in *Bn-clg1A-1D* transgenic *Arabidopsis*, epidermal cells at the base of petals are defective in cell elongation or delayed in their differentiation. On the opposite, petal mesophyll cells were more elongated in *Bn-clg1A-1D* transgenic *Arabidopsis* than in wild-type plants (see Supplemental Figures 11E and 11F online). Similarly, epidermal cells on the abaxial surface of the sepal were in general slightly more elongated and wider than their wild-type counterpart (Figures 8C and 8D; see Supplemental Figures 12G and 12H online).

No significant differences were observed in the number of epidermal cells at the abaxial surface of sepal and both abaxial and adaxial surfaces of petals. In square areas of $10,000 \mu\text{m}^2$, wild-type plants of *Arabidopsis* show 7.33 ± 1.17 and 9.23 ± 0.76 cells, whereas *Bn-clg1A-1D* transgenic *Arabidopsis* showed 9.07 ± 1.17 and 10.67 ± 1.55 cells for the abaxial and adaxial of

surfaces, respectively, of petal blades. Nevertheless, we observed that cells of the *Bn-clg1A-1D* transgenic plants were strongly misshapen (Figures 8E to 8H; see Supplemental Figure 12 online). Abaxial epidermal cells of the petal blade were more prominent and less inflated than wild-type cells (Figures 8E and 8F; see Supplemental Figures 12A and 12B online).

Interestingly, cuticular nanoridges, typically displayed on wild-type petal and sepal epidermis (Li-Beisson et al., 2009; Shi et al., 2011), were absent (petals) or severely reduced (sepals) at the abaxial surface of epidermal cells in the *Bn-clg1A-1D* transgenic *Arabidopsis* (Figures 8E to 8H; see Supplemental Figures 12G and 12H online). On the adaxial surface of petals, epidermal cells of *Bn-clg1A-1D* transgenic *Arabidopsis* were less conical and their flattened tips were deprived of nanoridges (see Supplemental Figures 12E and 12F online). Remarkably, abaxial surface of sepals appeared cracked or wrinkled because most of epidermal cells were hardly distinguishable and completely lost their tubular shapes (Figures 8G and 8H). Some surface areas exhibit wild-type cells with regular shapes, notably at the base of sepals.

DISCUSSION

In this study, we showed that a point mutation in a RINGv E3 ubiquitin ligase encoding gene (*Bn-CLG1A*) leads to cleistogamy phenotype in *B. napus*. The existence of *Bn-CLG1A* homologs in all eukaryotes suggests that their function is evolutionarily conserved. Biochemical and cellular characterization have shown that human (TEB4p) and yeast (DOA10p) homologs play a role in endoplasmic reticulum-associated degradation where ubiquitinylation is essential for both their retrotranslocation into the

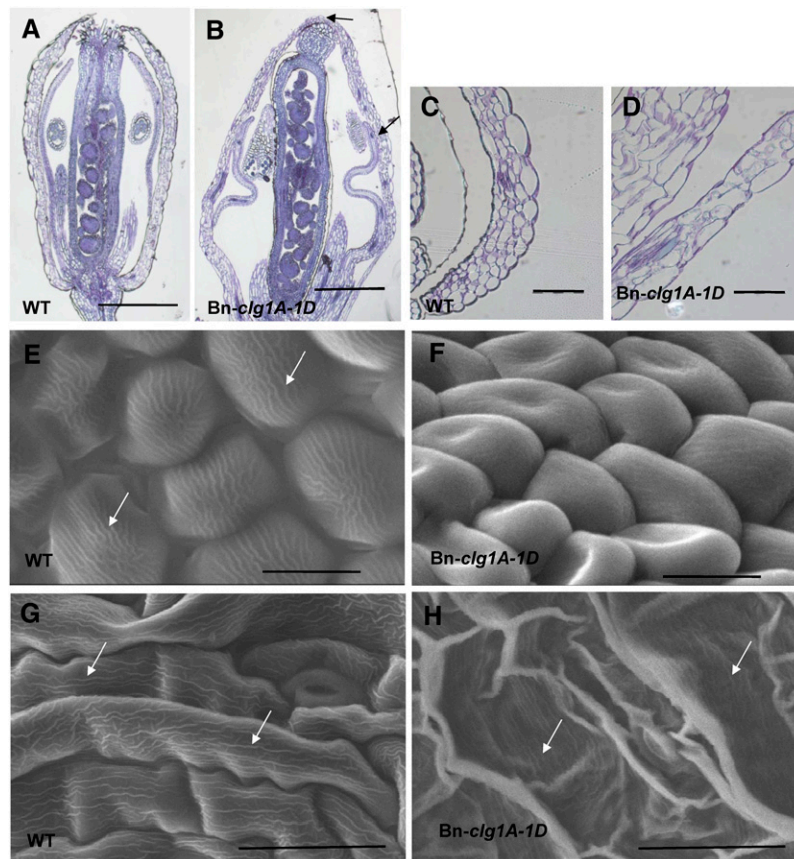


Figure 8. Changes in Flower Morphology and Surface Characteristics of *Arabidopsis* Plants Transformed with *Bn-clg1A-1D* as Observed by Light and Electron Microscopy.

(A) to (D) Light microscopy images of Toluidine Blue–stained longitudinal sections of flowers at developmental stage 12 [(A) and (B)] and sepals at developmental stage 13 [(C) and (D)]. Col-0 wild-type (WT) [(A) and (C)] and transgenic *Bn-clg1A-1D* plants [(B) and (D)] are represented. Arrows indicate sepal-to-sepal and sepal-to-petal fusions.

(E) to (H) Scanning electron microscopy images of abaxial surfaces of petal [(E) and (F)] and sepal [(G) and (H)] epidermis in Col-0 wild-type [(E) and (G)] and transgenic *Bn-clg1A-1D* plants [(F) and (H)]. Arrows indicate nanoridges.

Bars = 500 μ m in (A) and (B), 100 μ m in (C) and (D), 10 μ m in (E) and (F), and 30 μ m in (G) and (H).

[See online article for color version of this figure.]

cytosol and degradation (Swanson et al., 2001; Hwang et al., 2010). The Cri-du-chat syndrome, a neurodegenerative disorder in humans, was found to be associated with the chromosome region containing the *TEB4* gene (Hassink et al., 2005). The high protein structure conservation suggests that Bn-CLG1A should maintain a similar biochemical and cellular function in endoplasmic reticulum–associated degradation and ubiquitin-mediated protein degradation.

Bn-CLG1A and its homologs in plants exhibit specific evolutionary features: (1) The putative chloroplast/plastid targeting polypeptide signal in the N terminus of Bn-CLG1A homologs is highly conserved in eudicot plant species and was not found in fungi and animals and more interestingly not evidenced in the monocot grass plant species. (2) Moreover, the occurrence of a 23–amino acid domain is highly conserved among all the analyzed vascular and nonvascular plant species and that we called the cleistogamy domain. The P325L cleistogamy-inducing

point mutation in *B. napus* *Bn-clg1A-1D* occurred in this domain.

Interestingly, *B. napus* and *Arabidopsis* plants transformed with the *Bn-clg1A* gene showed cleistogamous flowers. The cleistogamy phenotype in these transgenic plants is most likely caused by the P325L mutation and not by other possible effects that would be independent from the mutation, such as overexpression of the *Bn-clg1A-1D* gene: (1) Transformation experiments were done in this study using a construct where the *Bn-clg1A-1D* gene is under the control of its endogenous promoter and not, for example, under the control of the 35S promoter, which favors overexpression. However, it could not be completely excluded that more or overexpression of the *Bn-clg1A-1D* transgene occurred under its endogenous promoter, as its expression was not analyzed in this study. (2) Nevertheless, overexpression is unlikely to cause the cleistogamy phenotype. The transformation and overexpression in *Arabidopsis*

of the *Arabidopsis* orthologous wild-type allele (*cer9*), which does not contain the P325L mutation, was done in a separate study (Lü et al., 2012), and no effect on flower morphology or cleistogamy phenotype was noticed. (3) Finally, *B. napus* noncleistogamous cultivars, having thus the two wild-type homoeologs, Bn-*CLG1A* and Bn-*CLG1C*, show normal flower phenotype.

During flower bud opening, various events take place, representing all aspects of plant development, such as cell division, cellular differentiation, and cell elongation or expansion. Flower opening depends on many factors, including internal ones, such as plant growth regulators (phytohormones), water supply, carbohydrate metabolism, cell wall/membrane metabolism, as well as external factors, such as light, temperature, and humidity (Kumar et al., 2008). The mechanism of flower opening varies considerably in the angiosperms (reviewed in van Doorn and van Meeteren, 2003). For some plant species, flower opening could be related to the development of adjacent tissues. For example, it may require growth of the pedicel or forced separation or abscission of covering parts. Flower opening can also depend on petal movements, which might be due to (1) reversible ion accumulation (independent from elongation growth), (2) cellular death in a specific area of the petal, (3) loss of water during the day and refilling during the night, and (4) differential growth rate of the two sides of the petal (as reviewed by van Doorn and van Meeteren, 2003). In most species, petal movements are due to a difference in growth rate of the two sides. In *Arabidopsis*, the opening of flower buds appears to be the result of rapid cell expansion (instead of cell division) in petals (primarily of the basal epidermal and mesophyll cells) (Pyke and Page, 1998). In grasses, like rice and barley, flower opening is achieved by a mechanism of lodicule (equivalent to petals in dicotyledons) swelling (Yoshida et al., 2007; Nair et al., 2010).

In this study, we have characterized several features of *Arabidopsis* Bn-*clg1A-1D* transgenic cleistogamous flowers that highlight important insights about the mechanism by which the P325L mutation leads to the cleistogamy phenotype. (1) We showed that expression of Bn-*clg1A-1D* causes petal-to-sepal and sepal-to-sepal fusions. Interestingly, *Arabidopsis* mutant lines, reported in other studies as affected in the flower phenotype, show also similar flower organ fusions (Li-Beisson et al., 2009; Panikashvili et al., 2009, 2011; Shi et al., 2011). Also, flower organ fusions, consisting of the formation of lodicule-glume mosaic organs, have been observed in cleistogamous flowers of rice (Yoshida et al., 2007). (2) We observed that Bn-*clg1A-1D* expression perturbed petal and sepal cell elongation, cellular expansion, and/or differentiation. Compared with wild-type plants, sepals epidermal and petal mesophyll cells of *Arabidopsis* Bn-*clg1A-1D* transgenic cleistogamous flowers were more elongated while epidermal cells at the base of petal were less elongated. (3) More importantly, we observed reduction of cuticular nanoridges on sepal and petal epidermal cells in cleistogamous *Arabidopsis* flowers, indicating defects in cutin loading or synthesis in flowers. Strikingly, similar defects in the synthesis or loading of cutin monomers was previously observed for other *Arabidopsis* lines that were independently reported as being affected in flower morphology (Li-Beisson et al., 2009; Panikashvili et al., 2009; Panikashvili et al., 2011; Shi et al., 2011).

Interestingly, a recent study has suggested that the orthologous *At4g34100* (*CER9*) wild-type gene of *Arabidopsis* acts as a negative regulator of cutin biosynthesis or loading (Lü et al., 2012). This was based on the fact that *cer9* recessive and loss-of-function mutants, corresponding to wax mutant *eceriferum9* (Koorneef et al., 1989), showed an elevated amount of cutin monomer (Lü et al., 2012). On the opposite side, the P325L cleistogamy mutation in *B. napus* Bn-*clg1A-1D* might cause a defect or reduction in cutin loading or synthesis in flowers as suggested by the observed reduction in petal and sepal cuticular nanoridges. These data strongly suggest that the mutant gene acts as a pronounced negative regulator of cutin biosynthesis or loading. Notably, no defect in flower morphology was reported for the *cer9* recessive and loss-of-function mutants (Koorneef et al., 1989; Lü et al., 2012). This was also the case for one *Arabidopsis* knockout line, mutated by T-DNA in the *At4g34100* gene, and two other lines transformed with RNA interference constructs that we have phenotyped (data not shown). Measurement of cuticular wax composition in Bn-*clg1A-1D* flowers will better shed light on how the P325L mutation affects the Bn-*CLG1A* function.

Together, these observations and comparisons with other studies strongly suggest that the P325L cleistogamy mutation Bn-*clg1A-1D* causes a pronounced negative regulation of cutin biosynthesis or loading and affects elongation or differentiation of petal and sepal cells. This probably results in inhibition or delay of the petal development as well as petal-to-sepal and sepal-to-sepal fusions, leading to folded petals and the cleistogamy phenotype. Accordingly, results from promoter-GUS analysis indicate that the Bn-*CLG1A* gene might function preferentially in petal, sepal, and stamen during flower development. No defect in leaf morphology or plant development was observed (data not shown). Intriguingly, quantitative RT-PCR analyses showed that Bn-*CLG1A* is constitutively expressed in all plant organs. Differences in protein-protein interactions depending on tissue-specific expression of the Bn-*clg1A* protein may explain this discrepancy. Alternatively, the P325L mutation at the cleistogamy domain may specifically affect flower development.

The P325L cleistogamy mutation in Bn-*clg1A-1D* did not affect its expression or that of its homoeologous Bn-*CLG1C* gene copy, suggesting that it acts at the protein interaction level. Moreover, heterozygous oilseed rape lines as well as transgenic *Arabidopsis* and oilseed rape plants expressing Bn-*clg1A-1D* exhibited a cleistogamous phenotype (Figures 1 and 3; Renard and Tanguy, 1997). These observations suggest that the P325L mutation is semidominant and not a loss-of-function mutation.

It is unlikely that the P325L mutation would correspond to a dominant-negative form. As discussed above, the *Arabidopsis* orthologous *CER9* gene was shown to act as a negative regulator of cutin loading or biosynthesis, (Lü et al., 2012). Therefore, if the P325L mutation is a dominant-negative form and alters this function (of negative regulation of cutin loading), we would expect to have more cutin monomer (and cuticular wax) in *Arabidopsis* transgenic plants. In contrast with this, we observed a marked and a more pronounced reduction of cuticular nanoridges in petals and sepals. Moreover, we didn't observe brighter leaves, stem, or silique phenotypes characteristic of *cer9* knockout

mutants (Koorneef et al., 1989). Therefore, the P325L mutation is functional and would rather correspond to a gain-of-function and semidominant positive form.

Various interpretations could be advanced to explain functionality of the gain of function and semidominant mutation of Bn-*clg1A-1D* in relation to the homoeologous Bn-*CLG1C*. A primary interpretation is that Bn-*CLG1A* and Bn-*CLG1C* wild-type homoeologous genes had established different and independent functions in *B. napus*, prior to the cleistogamy mutation. In this case, the semidominant P325L EMS mutation in the Bn-*CLG1A* homoeologous gene copy has led to the gain of function of the Bn-*clg1A-1D* cleistogamy allele, without any interaction with the Bn-*CLG1C* homoeologous gene. Sequence comparisons showed that Bn-*CLG1A* or Bn-*CLG1C* homoeologous genes in *B. napus* are 100% identical at the amino acid level to their corresponding orthologs in the *B. rapa* (Br-*CLG1A*) and *B. oleracea* (Bo-*CLG1C*) parental species. This suggests that no specific mutations or changes have occurred in *B. napus* to diverge the function of these homoeologous genes. This leaves a possibility that different functions preexisted and would have evolved in the Br-*CLG1A* or Bo-*CLG1C* orthologous genes of the parental species, before the recent allopolyploidy reunited them in the *B. napus* genome. This is also unlikely because the Br-*CLG1A* gene of *B. rapa* and its orthologous Bo-*CLG1C* gene of *B. oleracea*, which are highly conserved (99.5% identical at the amino acid sequence level), represent the unique genes of these parental species whose structure is highly conserved with Bn-*CLG1A* and Bn-*CLG1C* homoeologous genes of *B. napus*.

Therefore, the most plausible interpretation is that Bn-*CLG1A* and Bn-*CLG1C* of *B. napus* are functionally redundant. Functionally redundant duplicated genes can follow one of many possible evolutionary fates, including nonfunctionalization (deletion or pseudogenization of one duplicated copy), neofunctionalization (evolution of novel functions among alleles or homoeoalleles), or subfunctionalization (evolution of partitioned ancestral functions among alleles or homoeoalleles) (Lynch and Force, 2000; Prince and Pickett, 2002). Subfunctionalization and neofunctionalization were suggested as mechanisms leading to the preservation of duplicated genes after polyploidization (Lynch and Force, 2000; Prince and Pickett, 2002), and several interesting examples have been recently reported (Hovav et al., 2008; Chaudhary et al., 2009; Zhang et al., 2011). Although the cleistogamy mutation studied here is EMS induced and didn't occur during natural evolution as originally defined for sub- and neofunctionalization (Lynch and Force, 2000), our study provides an interesting example of functional and concerted interaction between two homoeologous genes in the relatively recent allopolyploid *B. napus*. The possible interaction fates are as follows: (1) The fact that the P325L cleistogamy mutation is not a loss-of-function or a recessive but rather a gain-of-function and semidominant positive mutation (see above) excludes the possibility that it led to loss of function of Bn-*CLG1A-1D*. (2) It is possible that this mutation may have caused an increased contribution of the Bn-*clg1A-1D* gene to the original function. We previously suggested this type of subfunctionalization, where a homoeologous gene contributes more to the function than the other ones, and defined it as hyperfunctionalization in the case of the domestication Q gene homoeologs in polyploid wheat (Zhang et al., 2011).

The hyperfunctionalization suggested here would act at the protein level and is supported by the finding that compared with the *At4g34100* wild-type (*CER9*) orthologous gene of *Arabidopsis*, which acts as a negative regulator of cutin biosynthesis or loading (Lü et al., 2012), the Bn-*clg1A-1D* cleistogamy mutant acts as a stronger negative regulator of cutin biosynthesis or loading. (3) On the other hand, neofunctionalization could also represent an alternate model for the interaction between the Bn-*clg1A-1D* gain-of-function semidominant mutation and its homoeologous Bn-*CLG1C* gene. The mutation didn't affect expression of the *clg1A* gene or of Bn-*CLG1C*. Moreover, the cleistogamy phenotype was observed independently from the copy number of homoeologs or homologs of the *clg1A* gene, present in the mutated *B. napus* as well as the transgenic *B. napus* and *Arabidopsis* in which Bn-*clg1A-1D* was introduced. These features characterize neofunctionalization (Lynch and Force, 2000).

Notably, whether Bn-*clg1A-1D* has been hyper- or neofunctionalized or has been subjected to a combination of both phenomena, it is not demonstrated in this study that the P325L mutation has impacted preservation of duplicated gene copies (Lynch and Force, 2000), although reproductive fitness and fertility of cleistogamous *B. napus* were not affected (Renard and Tanguy, 1997; Fargue et al., 2006).

In conclusion, our study reports the cloning of a cleistogamy gene in dicots that may cause pronounced negative regulation of cutin biosynthesis or loading in flower organs and corresponds to a gain of function in a homoeologous gene. Further detailed analyses are needed to determine the cutin monomer composition in cleistogamous flowers as well as to identify Bn-*CLG1A* and Bn-*clg1A* interacting proteins. Analysis of the Bn-*CLG1A* and Bn-*clg1A* E3 ligase activity also would be interesting. The study opens new perspectives for future characterizations of the biological functions of Bn-*CLG1A* as well as the fate of duplicated genes and the evolution of new functions of duplicated gene copies in allopolyploid species.

METHODS

Plant Materials

The *Brassica napus* cleistogamous mutant was originally obtained in the seventies at Institut National de la Recherche Agronomique Rennes by EMS mutagenesis on seeds of the cv Primor (Renard and Tanguy, 1997). The cleistogamous trait was then introduced into the cultivar 'Samourai' by successive backcrossing, and this gave rise to the cleistogamous line 'B001-*Clg*' used as the cleistogamous parent in this study.

A population of 255 DH lines was produced by microspore culture from the F1 plants of a cross between 'Yudal' (open flower type) and 'B001-*Clg*' (cleistogamous type) as described by Polsoni et al. (1988) and used for initial mapping of Bn-*clg1A-1D*. All the DH lines were first phenotyped twice in greenhouse for cleistogamy. These were also evaluated in the experimental field conditions of Institut National de la Recherche Agronomique Le Rheu (Rennes, France) and used for the initial AFLP mapping. For fine mapping, a total of 2158 DH lines were genotyped with linked molecular markers, and 31 recombinant lines were then evaluated for the cleistogamy phenotype in the field and greenhouse conditions.

Arabidopsis thaliana plants were grown on soil in a greenhouse at 22°C/16-h day and 18°C/8-h night cycle. *B. napus* plants were grown either in

the field or in a greenhouse with a thermo/photoperiod of 25°C/16-h days and 18°C/8-h nights.

For expression analysis, plants of *B. napus* cv Darmor were individually planted into 2-liter pots filled with perlite. Plants were regularly watered with Hoagland nutritive solution. Root samples were collected from 6-week-old plants. Leaf blades and petioles separated from the three younger leaves and stem sections at the base of plants were sampled on 2-month-old plants. Young floral buds as well as young siliques and immature seeds at 11 and 19 d after manual pollination, respectively, were collected on 3.5-month-old plants. For *B. napus* cv Primor and Primor-*Clg* winter cultivars, 3 weeks after planting in soil, plants were vernalized for 2 months at 8°C with a 16-h/8-h day/night conditions. After 1 month of growth in the greenhouse, 3- to 5-mm floral buds were collected. All samples were immediately frozen in liquid nitrogen upon collection. For each sample, at least three individual plants were pooled together.

Methods of phenotyping, molecular marker development, DNA extraction, and fine genetic mapping of Bn-*clg1-1D* are detailed in Supplemental Methods 1 online.

Construction and Screening of Ordered and Pooled BAC Libraries

A BAC genomic DNA library was previously constructed from cv Darmor-*Bzh* (Chalhoub et al., 2004). This was used for physical mapping of Bn-*CLG1A* where the BAC clone CZ7N2 containing Bn-*CLG1A* was identified.

To isolate the mutant allele Bn-*clg1A-1D*, we constructed a pooled large insert library for Primor-*Clg* cultivar following the procedures described by Isidore et al. (2005). Specific PCR markers tightly linked to Bn-*clg1A-1D* were then used to screen the pools of BAC clones of the library to identify the BAC clone "Clg_H1B_P13a_3_J1" containing the mutant allele.

Sequence Alignment and Phylogenetic Analysis of Bn-*CLG1A* Homologs

BAC clone sequencing and annotation were done as essentially described by Chantret et al. (2005). Multiple sequence alignments were performed with ClustalX (Thompson et al., 1997). The protein sequences of Bn-*CLG1A* homologs in other species were retrieved by TBLASTp search from the "nonredundant protein sequences" databases at the National Center for Biotechnology Information (<http://www.ncbi.nlm.nih.gov/BLAST/>). The evolutionary distances were computed using the Poisson correction method (Zuckerkanndl and Pauling, 1965). Phylogenetic analyses were conducted with MEGA4 software (Tamura et al., 2007), where the software option relying on the neighbor-joining method (Saitou and Nei, 1987) was applied. A bootstrap test inferred from 1000 replicates was applied (Felsenstein, 1985).

Analysis and Comparison of Protein Sequence Domains

Subcellular localization of the different protein sequences were predicted by the online software WoLFPSORT (<http://wolfsort.org/>), MultiLoc (<http://www.bs.informatik.uni-tuebingen.de/Services/MultiLoc/>), TargetP1.1 (<http://www.cbs.dtu.dk/services/TargetP/>), ChloroP 1.1, (<http://www.cbs.dtu.dk/services/ChloroP/>), TargetLoc (<http://www.bs.informatik.uni-tuebingen.de/Services/MultiLoc/>), PredictNL (<http://cubic.bioc.columbia.edu/cgi/var/nair/resonline.pl>), and LOCTree (<http://cubic.bioc.columbia.edu/cgi-bin/var/nair/loc>). Membrane topology of Bn-*CLG1A*, TEB4p, and DAO10p was predicted by TMHMM2.0 (<http://www.cbs.dtu.dk/services/TMH/>) (Krogh et al., 2001).

Gene Expression Analysis

Total RNA was extracted using Trizol reagent (Invitrogen) for Darmor samples or using the SV Total RNA isolation kit (Promega) for Primor and

Primor-*Clg* samples according to the manufacturers' instructions. Genomic DNA was removed by digestion with DNase I (RNase-free; Ambion) according to the manufacturer's protocol except that DNase I was heat inactivated by 5-min incubation at 75°C. RNA concentration and integrity were determined by OD measurement at 260 and 280 nm and with an Agilent 2100 Bioanalyzer (Agilent Technologies). Two micrograms of total RNA were reverse transcribed using 500 ng of oligo(dT)12-18 and 200 units of SuperScriptII RT in a total volume of 20 μ L following the manufacturer's instructions (Invitrogen, Life Technologies). After first-strand cDNA synthesis, RNA complementary to the cDNA was removed by incubating the reaction with 2 units of *Escherichia coli* RNase H at 37°C for 20 min. cDNA was diluted fivefold before real-time PCR. Real-time PCR reactions were performed on a CFX384 Touch Real-Time PCR detection system (Bio-Rad) using 9 μ L of SsoAdvanced SYBR Green Supermix (Bio-Rad), 2 μ L of cDNA, and 0.56 μ M primers in a total volume of 18 μ L per reaction. The cycling conditions were composed of an initial 30-s denaturation step at 95°C, followed by 40 cycles of 95°C for 5 s and 60°C for 30 s. Melting curve was run from 65 to 95°C to ensure the specificity of product. Data were analyzed using CFX Manager Software version 2.1 (Bio-Rad). *B. napus* elongation factor 1 (*EF-1*) and ubiquitin 2 (*UBQ2*) were used as reference genes for normalization of gene expression levels in all samples. Quantitative RT-PCR forward and reverse primer sequences for each gene are listed in Supplemental Table 1 online. Primer efficiencies for each couple of primers were 95.57% for Bn-*CLG1A*, 101.52% for Bn-*CLG1C*, 91.79% for *EF-1*, and 91.07% for *UBQ2*.

Gene Constructs, Transformations, and Complementation Analysis

To validate function of the cleistogamy candidate gene, two constructs were used. The pBn-clg1A:Bn-clg1A construct (see Supplemental Figure 9 online) contains an *Xba*I-generated 5999-bp genomic fragment of the mutant allele cloned into the binary vector pBINPLUS (van Engelen et al., 1995). The 5999-bp genomic fragment is composed of a 895-bp native promoter region, the 4144-bp predicted coding Bn-*clg1A-1D* allele, and the 960-bp downstream 3'-untranslated region (see Supplemental Figure 9 online). The pBn-clg1A:GUS construct was made using the 893-bp fragment of the promoter region of the candidate Bn-*CLG1A* gene (see Supplemental Figure 9 online) inserted at the beginning of GUS gene, into a binary vector pBI101-GUS with Gateway cloning technology (Invitrogen). We conducted *Agrobacterium tumefaciens*-mediated transformations in oilseed rape using methods developed by Moloney et al. (1989) and Sparrow et al. (2004) and in *Arabidopsis* by floral dip according to Clough and Bent (1998). Transgenic T1 plants were selected on half-strength Murashige and Skoog media containing 50 μ g/mL kanamycin. pBn-clg1A:GUS construct was used for GUS coloration assays (Jefferson et al., 1987) to check specificity of expression in the different tissues of transformed *B. napus*.

Microscopy

For Toluidine Blue-O staining, the inflorescences of 7-week-old plants were fixed in a 1% glutaraldehyde, 2% paraformaldehyde, and 1% caffeine solution and embedded in Kulser resin. Sections were cut to a thickness of 5 μ m on a microtome before Toluidine Blue-O staining. For scanning electron microscopy analysis, flowers from 7-week-old plants were collected, and samples were slowly frozen at -30°C under a partial vacuum on the Peltier stage before observation using a Hirox SH-1500 microscope at 15 kV.

Accession Numbers

Sequence data from this article can be found in the Arabidopsis Genome Initiative or GenBank/EMBL databases under the following accession

numbers: BAC clone CZ7N2, KC206509; BAC clone Clg_H1B_P13a_3_J1, KC206510; Bn-*CLG1A*, KC206501; Bn-*clg1A-1D*, KC206502; Bn-*CLG1C*, KC206503; Bn-*Rzfp2A*, KC206504; Bn-*Rzfp2C*, KC206505; Bn-*Rzfp3A*, KC206506; Bn-*Rzfp3C*, KC206507; Bn-*Rzfp2Cb*, KC206508; *EF1*, *FJ529180*; *UBQ2*, *EE426322*; *CER9*, *At4G34100*. The other *Brassica* sequence data are from the BRAD database (<http://brassicadb.org/brad/>) and have the following accession numbers: Bo-*CLG1C*, BGIContig_196373_816_7400_rv; Bo-*Rzfp2C*, BGIscaf7180014794361_6919537_6925790_rv; Bo-*Rzfp2Cb*, BGIscaf7180014794480_102891_108258_rv; Bo-*Rzfp3C*, BGIscaf7180014794480_67182_72615_rv; Br-*CLG1A*, Bra011487 or BGIScaffold000011_2395792_2402090; Br-*Rzfp2A*, BGIScaffold000023_175528_181823; Br-*Rzfp3A*, BGIScaffold000097_438462_443628. From GenBank (<http://www.ncbi.nlm.nih.gov/>), accession numbers of sequence data for Bn-*CLG1A* homologs of other species used in this study are supplied in Supplemental Table 4 online.

Supplemental Data

The following materials are available in the online version of this article.

Supplemental Figure 1. Scoring and Segregation of the Cleistogamy Phenotype in a Population of 255 Doubled Haploid Lines of *B. napus*.

Supplemental Figure 2. Dot Plot Comparison between the *Brassica napus* Region Spanning the Bn-*CLG1A* Wild-Type Gene and the Orthologous Genomic Sequence from *Arabidopsis thaliana*.

Supplemental Figure 3. Physical Positions of the Genetic Markers Closely Linked to Bn-*CLG1A* and Sequence Comparison between Bn-*CLG1A* and Bn-*clg1A-1D*.

Supplemental Figure 4. Design of a dCAPS Marker for the Detection of the T/C SNP Differentiating Bn-*clg1A-1D* and Bn-*CLG1A*.

Supplemental Figure 5. Chromosomal Colinearity and Phylogenetic Relationships between Genes from the *Arabidopsis* Chromosome 4 Genomic Region Spanning the *At4g34100* Gene and Their Triplicated Orthologs Found in *Brassica rapa*.

Supplemental Figure 6. Phylogenetic Analysis of Homologs of Bn-*CLG1A*.

Supplemental Figure 7. Alignment of RINGv Domains of Bn-*CLG1A* Homologous Protein Sequences Identified in All Eukaryote Species.

Supplemental Figure 8. Comparison of Membrane Topology between Bn-*CLG1A* TEB4p and DOA10p Proteins.

Supplemental Figure 9. Schematic Presentation of Genomic DNA Promoter Fragments Used for the pBn-*CLG1A*:*GUS* Construct, as Well as the Entire Gene Sequence Fragment Used for Bn-*clg1A-1D* Gene-Derived Construct (pBn-*clg1-1D*).

Supplemental Figure 10. Reproductive Organ Morphology of *Arabidopsis* Plants Transformed with Bn-*clg1A-1D*.

Supplemental Figure 11. Light Microscopy of Toluidine Blue–Stained Sections of Wild-Type and Bn-*clg1A-1D* Flowers.

Supplemental Figure 12. Scanning Electron Microscopy of *Arabidopsis* Bn-*clg1A-1D* Transgenic Plants.

Supplemental Table 1. Primers Used for Genetic Mapping and Quantitative PCR.

Supplemental Table 2. Comparison of Gene Content between the *Brassica napus* BAC Clone CZ7N2 and the Corresponding Region of *Arabidopsis* Chromosome 4.

Supplemental Table 3. Bn-*clg1A-1D*/ Bn-*CLG1A* Near-Isogenic Lines and Representative Oilseed Rape Cultivars Analyzed by the dCAPS_Clg1 Marker.

Supplemental Table 4. Bn-*clg1A-1D* Orthologs Used for Phylogenetic Tree Construction in Figure 5 and Supplemental Figure 6.

Supplemental Data Set 1. Test File of Alignment Used to Generate Phylogenetic Tree in Figure 5.

Supplemental Data Set 2. Test File of Alignment Used to Generate Phylogenetic Tree in Supplemental Figure 6.

Supplemental Results 1. Detailed Description of the Positional Cloning of Bn-*CLG1A*.

Supplemental Methods 1. Phenotyping, Molecular Marker Development, DNA Extraction, and Fine Genetic Mapping of Bn-*CLG1A*.

ACKNOWLEDGMENTS

This work was supported by the French Genoplante (GOP-T2 and GOP-T7) projects (<http://www.genoplante.com/>). D.A. was supported by a Genopole-Evry postdoctorate fellowship. We thank Halima Morin and Nero Borrega from the Cytology and Cell Imaging Platform (Institut National de la Recherche Agronomique Versailles) for help with microscopy observations. We also thank France Denoeud from the Commissariat à l'Énergie Atomique-Genoscope (Evry, France) for help obtaining homologs of the Bn-*CLG1A* gene from different species.

AUTHOR CONTRIBUTIONS

Y.-H.L., D.A., R.D., and B.C. designed the project, conducted the experiments, and wrote the article. H.B., P.R., N.P., M.-O.L., and C.F. conducted experiments. J.J. conducted sequence analysis. M.R. contributed to the design of the project and to writing.

Received August 22, 2012; revised November 11, 2012; accepted December 5, 2012; published December 31, 2012.

REFERENCES

- Ammitzbøll, H., and Bagger Jørgensen, R. (2006). Hybridization between oilseed rape (*Brassica napus*) and different populations and species of *Raphanus*. *Environ. Biosafety Res.* **5**: 3–13.
- Beckie, H.J., Warwick, S.I., Nair, H., and Seguin-Swartz, G. (2003). Gene flow in commercial fields of herbicide-resistant canola (*Brassica napus*). *Ecol. Appl.* **13**: 1276–1294.
- Borden, K.L. (2000). RING domains: Master builders of molecular scaffolds? *J. Mol. Biol.* **295**: 1103–1112.
- Borden, K.L., and Freemont, P.S. (1996). The RING finger domain: A recent example of a sequence-structure family. *Curr. Opin. Struct. Biol.* **6**: 395–401.
- Carroll, S.B. (2001). Chance and necessity: The evolution of morphological complexity and diversity. *Nature* **409**: 1102–1109.
- Carvalho, P., Goder, V., and Rapoport, T.A. (2006). Distinct ubiquitin-ligase complexes define convergent pathways for the degradation of ER proteins. *Cell* **126**: 361–373.
- Chalhoub, B., Belcram, H., and Caboche, M. (2004). Efficient cloning of plant genomes into bacterial artificial chromosome (BAC) libraries with larger and more uniform insert size. *Plant Biotechnol. J.* **2**: 181–188.
- Chalhoub, B.A., Thibault, S., Laucou, V., Rameau, C., Höfte, H., and Cousin, R. (1997). Silver staining and recovery of AFLP amplification products on large denaturing polyacrylamide gels. *Biotechniques* **22**: 216–218, 220.

- Chantret, N., et al.** (2005). Molecular basis of evolutionary events that shaped the hardness locus in diploid and polyploid wheat species (*Triticum* and *Aegilops*). *Plant Cell* **17**: 1033–1045.
- Chaudhary, B., Flagel, L., Stupar, R.M., Udall, J.A., Verma, N., Springer, N.M., and Wendel, J.F.** (2009). Reciprocal silencing, transcriptional bias and functional divergence of homeologs in polyploid cotton (*Gossypium*). *Genetics* **182**: 503–517.
- Cheng, F., Wu, J., Fang, L., Sun, S., Liu, B., Lin, K., Bonnema, G., and Wang, X.** (2012). Biased gene fractionation and dominant gene expression among the subgenomes of *Brassica rapa*. *PLoS ONE* **7**: e36442.
- Chhabra, A.K., and Sethi, S.K.** (1991). Inheritance of cleistogamic flowering in durum wheat (*Triticum aestivum* L.). *Euphytica* **55**: 147–150.
- Clough, S.J., and Bent, A.F.** (1998). Floral dip: A simplified method for Agrobacterium-mediated transformation of *Arabidopsis thaliana*. *Plant J.* **16**: 735–743.
- Culley, T.M., and Klooster, M.R.** (2007). The cleistogamous breeding system: A review of its frequency, evolution, and ecology in angiosperms. *Bot. Rev.* **73**: 1–30.
- Daniell, H.** (2002). Molecular strategies for gene containment in transgenic crops. *Nat. Biotechnol.* **20**: 581–586.
- Darwin, C.** (1877). *The Different Forms of Flowers on Plants of the Same Species.* (London: John Murray).
- Fargue, A.N., Colbach, P.J., Picault, H., Renard, M., and Meynard, J.M.** (2006). Predictive study of the advantages of cleistogamy in oilseed rape in limiting unwanted gene flow. *Euphytica* **151**: 1–13.
- Felsenstein, J.** (1985). Confidence limits on phylogenies: An approach using the bootstrap. *Evolution* **39**: 783–791.
- Ford, C.S., Allainguillaume, J., Grilli-Chantler, P., Cuccato, G., Allender, C.J., and Wilkinson, M.J.** (2006). Spontaneous gene flow from rapeseed (*Brassica napus*) to wild *Brassica oleracea*. *Proc. Biol. Sci.* **273**: 3111–3115.
- Halfhill, M.D., Millwood, R.J., Raymer, P.L., and Stewart, C.N. Jr.** (2002). *Bt*-transgenic oilseed rape hybridization with its weedy relative, *Brassica rapa*. *Environ. Biosafety Res.* **1**: 19–28.
- Hampton, R.Y.** (2002). ER-associated degradation in protein quality control and cellular regulation. *Curr. Opin. Cell Biol.* **14**: 476–482.
- Hassink, G., Kikkert, M., van Voorden, S., Lee, S.J., Spaapen, R., van Laar, T., Coleman, C.S., Bartee, E., Früh, K., Chau, V., and Wiertz, E.** (2005). TEB4 is a C4HC3 RING finger-containing ubiquitin ligase of the endoplasmic reticulum. *Biochem. J.* **388**: 647–655.
- Hovav, R., Udall, J.A., Chaudhary, B., Rapp, R., Flagel, L., and Wendel, J.F.** (2008). Partitioned expression of duplicated genes during development and evolution of a single cell in a polyploid plant. *Proc. Natl. Acad. Sci. USA* **105**: 6191–6195.
- Hwang, C.S., Shemorry, A., and Varshavsky, A.** (2010). N-terminal acetylation of cellular proteins creates specific degradation signals. *Science* **327**: 973–977.
- Isidore, E., Scherrer, B., Bellec, A., Budin, K., Faivre-Rampant, P., Waugh, R., Keller, B., Caboche, M., Feuillet, C., and Chalhoub, B.** (2005). Direct targeting and rapid isolation of BAC clones spanning a defined chromosome region. *Funct. Integr. Genomics* **5**: 97–103.
- Jefferson, R.A., Kavanagh, T.A., and Bevan, M.W.** (1987). GUS fusions: β -Glucuronidase as a sensitive and versatile gene fusion marker in higher plants. *EMBO J.* **6**: 3901–3907.
- Jørgensen, R.B., and Andersen, B.** (1994). Spontaneous hybridization between oilseed rape (*Brassica napus*) and weedy *B. campestris* (Brassicaceae): A risk of genetically modified oilseed rape. *Am. J. Bot.* **81**: 1520–1526.
- Koorneef, M., Hanhart, C.J., and Thiel, F.** (1989). A genetic and phenotypic description of *Eceriferum* (*cer*) mutants in *Arabidopsis thaliana*. *J. Hered.* **80**: 118–122.
- Kraft, E., Stone, S.L., Ma, L., Su, N., Gao, Y., Lau, O.S., Deng, X.W., and Callis, J.** (2005). Genome analysis and functional characterization of the E2 and RING-type E3 ligase ubiquitination enzymes of *Arabidopsis*. *Plant Physiol.* **139**: 1597–1611.
- Kreft, S.G., Wang, L., and Hochstrasser, M.** (2006). Membrane topology of the yeast endoplasmic reticulum-localized ubiquitin ligase *Doa10* and comparison with its human ortholog *TEB4* (*MARCH-VI*). *J. Biol. Chem.* **281**: 4646–4653.
- Krogh, A., Larsson, B., von Heijne, G., and Sonnhammer, E.L.** (2001). Predicting transmembrane protein topology with a hidden Markov model: Application to complete genomes. *J. Mol. Biol.* **305**: 567–580.
- Kumar, N., Srivastava, G.C., and Dixit, K.** (2008). Flower bud opening and senescence in roses (*Rosa hybrida* L.). *Plant Growth Regul.* **55**: 81–99.
- Kurauchi, N., Makino, T., and Hirose, S.** (1993). Inheritance of cleistogamy-chasmogamy in barley. *Barley Genet. Newsl.* **23**: 19.
- Kwon, Y.W., Kim, D.S., and Yim, K.O.** (2001). Herbicide-resistant genetically modified crop: assessment and management of gene flow. *Weed Biol. Manage.* **1**: 42–51.
- Li-Beisson, Y., Pollard, M., Sauveplane, V., Pinot, F., Ohlogge, J., and Beisson, F.** (2009). Nanoridges that characterize the surfacemorphology of flowers require the synthesis of cutin polyester. *Proc. Natl. Acad. Sci. USA* **106**: 22008–22013.
- Lord, E.M.** (1981). Cleistogamy: A tool for the study of floral morphogenesis, function and evolution. *Bot. Rev.* **47**: 421–449.
- Lorick, K.L., Jensen, J.P., Fang, S., Ong, A.M., Hatakeyama, S., and Weissman, A.M.** (1999). RING fingers mediate ubiquitin-conjugating enzyme (E2)-dependent ubiquitination. *Proc. Natl. Acad. Sci. USA* **96**: 11364–11369.
- Lovering, R., Hanson, I.M., Borden, K.L., Martin, S., O'Reilly, N.J., Evan, G.I., Rahman, D., Pappin, D.J., Trowsdale, J., and Freemont, P.S.** (1993). Identification and preliminary characterization of a protein motif related to the zinc finger. *Proc. Natl. Acad. Sci. USA* **90**: 2112–2116.
- Lu, B.R.** (2003). Transgene containment by molecular means—Is it possible and cost effective? *Environ. Biosafety Res.* **2**: 3–8.
- Lü, S., Zhao, H., Des Marais, D.L., Parsons, E.P., Wen, X., Xu, X., Bangarusamy, D.K., Wang, G., Rowland, O., Juenger, T., Bressan, R.A., and Jenks, M.A.** (2012). *Arabidopsis ECRIFERUM9* involvement in cuticle formation and maintenance of plant water status. *Plant Physiol.* **159**: 930–944.
- Lynch, M., and Force, A.** (2000). The probability of duplicate gene preservation by subfunctionalization. *Genetics* **154**: 459–473.
- Lysak, M.A., Cheung, K., Kitzschke, M., and Bures, P.** (2007). Ancestral chromosomal blocks are triplicated in *Brassicaceae* species with varying chromosome number and genome size. *Plant Physiol.* **145**: 402–410.
- Maeng, J.Y., Won, Y.J., Piao, R., Cho, Y.I., Jiang, W., Chin, J.H., and Koh, H.J.** (2006). Molecular mapping of a gene '*ld(t)*' controlling cleistogamy in rice. *Theor. Appl. Genet.* **112**: 1429–1433.
- Merwin, N.C., Glurey, L.M., and Blackwell, K.H.** (1981). Inheritance of papery glume and cleistogamy in sorghum. *Crop Sci.* **21**: 953–956.
- Moloney, M.M., Walker, J.M., and Sharma, K.K.** (1989). High efficiency transformation of *Brassica napus* using *Agrobacterium* vectors. *Plant Cell Rep.* **8**: 238–242.
- Nair, S.K., et al.** (2010). Cleistogamous flowering in barley arises from the suppression of microRNA-guided *HvAP2* mRNA cleavage. *Proc. Natl. Acad. Sci. USA* **107**: 490–495.
- Panikashvili, D., Shi, J.X., Schreiber, L., and Aharoni, A.** (2009). The *Arabidopsis DCR* encoding a soluble BAHD acyltransferase is required for cutin polyester formation and seed hydration properties. *Plant Physiol.* **151**: 1773–1789.
- Panikashvili, D., Shi, J.X., Schreiber, L., and Aharoni, A.** (2011). The *Arabidopsis* ABCG13 transporter is required for flower cuticle secretion and patterning of the petal epidermis. *New Phytol.* **190**: 113–124.

- Parkin, I.A., Gulden, S.M., Sharpe, A.G., Lukens, L., Trick, M., Osborn, T.C., and Lydiate, D.J. (2005). Segmental structure of the *Brassica napus* genome based on comparative analysis with *Arabidopsis thaliana*. *Genetics* **171**: 765–781.
- Polsoni, L., Kott, S., and Beversdorf, W.D. (1988). Large-scale microspore culture technique for mutation selection studies in *Brassica napus*. *Can. J. Bot.* **66**: 1681–1685.
- Prince, V.E., and Pickett, F.B. (2002). Splitting pairs: The diverging fates of duplicated genes. *Nat. Rev. Genet.* **3**: 827–837.
- Pyke, K.A., and Page, A.M. (1998). Plastid ontogeny during petal development in *Arabidopsis*. *Plant Physiol.* **116**: 797–803.
- Renard, M., and Tanguy, X. (1997). Obtention de mutants cléistogames de crucifères. *Brevet FR 9715768*.
- Saitou, N., and Nei, M. (1987). The neighbor-joining method: A new method for reconstructing phylogenetic trees. *Mol. Biol. Evol.* **4**: 406–425.
- Saxena, K.B., Ariyanayagam, R.P., and Reddy, L.J. (1992). Genetics of a high-selfing trait in pigeonpea. *Euphytica* **59**: 2–3.
- Saxena, K.B., Singh, L., and Ariyanayagam, R.P. (1993). Role of partial cleistogamy in maintaining genetic purity of pigeonpea. *Euphytica* **66**: 225–229.
- Schemske, D.W. (1978). Evolution of reproductive characteristics in *Impatiens* (*Balsaminaceae*): The significance of cleistogamy and chasmogamy. *Ecology* **59**: 596–613.
- Shi, J.X., Malitsky, S., De Oliveira, S., Branigan, C., Franke, R.B., Schreiber, L., and Aharoni, A. (2011). SHINE transcription factors act redundantly to pattern the archetypal surface of *Arabidopsis* flower organs. *PLoS Genet.* **7**: e1001388.
- Schranz, M.E., and Mitchell-Olds, T. (2006). Independent ancient polyploidy events in the sister families *Brassicaceae* and *Cleomaceae*. *Plant Cell* **18**: 1152–1165.
- Silva, N.F., and Goring, D.R. (2001). Mechanisms of self-incompatibility in flowering plants. *Cell. Mol. Life Sci.* **58**: 1988–2007.
- Smalle, J., and Vierstra, R.D. (2004). The ubiquitin 26S proteasome proteolytic pathway. *Annu. Rev. Plant Biol.* **55**: 555–590.
- Song, X., Wang, Z., Zuo, J., Huangfu, C., and Qiang, S. (2010). Potential gene flow of two herbicide-tolerant transgenes from oilseed rape to wild *B. juncea* var. *gracilis*. *Theor. Appl. Genet.* **120**: 1501–1510.
- Sparrow, P.A.C., Townsend, T.M., Morgan, C.L., Dale, P.J., Arthur, A.E., and Irwin, J.A. (2004). Genetic analysis of in vitro shoot regeneration from cotyledonary petioles of *Brassica oleracea*. *Theor. Appl. Genet.* **108**: 1249–1255.
- Stone, S.L., Hauksdóttir, H., Troy, A., Herschleb, J., Kraft, E., and Callis, J. (2005). Functional analysis of the RING-type ubiquitin ligase family of *Arabidopsis*. *Plant Physiol.* **137**: 13–30.
- Swanson, R., Locher, M., and Hochstrasser, M. (2001). A conserved ubiquitin ligase of the nuclear envelope/endoplasmic reticulum that functions in both ER-associated and *Matalpha2* repressor degradation. *Genes Dev.* **15**: 2660–2674.
- Takahashi, R., Kurosaki, H., Yumoto, S., Han, O.K., and Abe, J. (2001). Genetic and linkage analysis of cleistogamy in soybean. *J. Hered.* **92**: 89–92.
- Tamura, K., Dudley, J., Nei, M., and Kumar, S. (2007). MEGA4: Molecular Evolutionary Genetics Analysis (MEGA) software version 4.0. *Mol. Biol. Evol.* **24**: 1596–1599.
- Tang, H., Woodhouse, M.R., Cheng, F., Schnable, J.C., Pedersen, B.S., Conant, G., Wang, X., Freeling, M., and Pires, J.C. (2012). Altered patterns of fractionation and exon deletions in *Brassica rapa* support a two-step model of paleohexaploidy. *Genetics* **190**: 1563–1574.
- Thompson, J.D., Gibson, T.J., Plewniak, F., Jeanmougin, F., and Higgins, D.G. (1997). The CLUSTAL_X windows interface: Flexible strategies for multiple sequence alignment aided by quality analysis tools. *Nucleic Acids Res.* **25**: 4876–4882.
- Turuspekov, Y., Mano, Y., Honda, I., Kawada, N., Watanabe, Y., and Komatsuda, T. (2004). Identification and mapping of cleistogamy genes in barley. *Theor. Appl. Genet.* **109**: 480–487.
- Uphof, J.C.T. (1938). Cleistogamic flowers. *Bot. Rev.* **4**: 21–49.
- van Doorn, W.G., and Van Meeteren, U. (2003). Flower opening and closure: A review. *J. Exp. Bot.* **54**: 1801–1812.
- van Engelen, F.A., Molthoff, J.W., Conner, A.J., Nap, J.P., Pereira, A., and Stiekema, W.J. (1995). pBINPLUS: An improved plant transformation vector based on pBIN19. *Transgenic Res.* **4**: 288–290.
- Vierstra, R.D. (2009). The ubiquitin-26S proteasome system at the nexus of plant biology. *Nat. Rev. Mol. Cell Biol.* **10**: 385–397.
- von Heijne, G., Steppuhn, J., and Herrmann, R.G. (1989). Domain structure of mitochondrial and chloroplast targeting peptides. *Eur. J. Biochem.* **180**: 535–545.
- Vos, P., Hogers, R., Bleeker, M., Reijans, M., van de Lee, T., Hornes, M., Frijters, A., Pot, J., Peleman, J., Kuiper, M., and Zabeau, M. (1995). AFLP: A new technique for DNA fingerprinting. *Nucleic Acids Res.* **23**: 4407–4414.
- Waller, D.M. (1984). Differences in fitness between seedlings derived from cleistogamous and chasmogamous flowers in *Impatiens capensis*. *Evolution* **38**: 427–440.
- Wang, X., et al; *Brassica rapa* Genome Sequencing Project Consortium (2011). The genome of the mesopolyploid crop species *Brassica rapa*. *Nat. Genet.* **43**: 1035–1039.
- Warwick, S.I., Simard, M.J., Légère, A., Beckie, H.J., Braun, L., Zhu, B., Mason, P., Séguin-Swartz, G., and Stewart, C.N. Jr. (2003). Hybridization between transgenic *Brassica napus* L. and its wild relatives: *Brassica rapa* L., *Raphanus raphanistrum* L., *Sinapis arvensis* L., and *Erucastrum gallicum* (Willd.) O.E. Schulz. *Theor. Appl. Genet.* **107**: 528–539.
- Yoshida, H., Itoh, J.I., Ohmori, S., Miyoshi, K., Horigome, A., Uchida, E., Kimizu, M., Matsumura, Y., Kusaba, M., Satoh, H., and Nagato, Y. (2007). *superwoman1*-cleistogamy, a hopeful allele for gene containment in GM rice. *Plant Biotechnol. J.* **5**: 835–846.
- Zhang, Z., et al. (2011). Duplication and partitioning in evolution and function of homoeologous Q loci governing domestication characters in polyploid wheat. *Proc. Natl. Acad. Sci. USA* **108**: 18737–18742.
- Zuckerandl, E., and Pauling, L. (1965). Evolutionary divergence and convergence in proteins. In *Evolving Genes and Proteins*, V. Bryson and H.J. Vogel, eds (New York: Academic Press), pp. 97–166.
- Zybailov, B., Rutschow, H., Friso, G., Rudella, A., Emanuelsson, O., Sun, Q., and van Wijk, K.J. (2008). Sorting signals, N-terminal modifications and abundance of the chloroplast proteome. *PLoS One* **3**: e1994.